



**QUEEN'S  
UNIVERSITY  
BELFAST**

## **Microbial community of the deep-sea brine Lake Kryos seawater-brine interface is active below the chaotropy limit of life as revealed by recovery of mRNA**

Yakimov, M. M., La Cono, V., Spada, G. L., Bortoluzzi, G., Messina, E., Smedile, F., Arcadi, E., Borghini, M., Ferrer, M., Schmitt-Kopplin, P., Hertkorn, N., Cray, J. A., Hallsworth, J. E., Golyshin, P. N., & Giuliano, L. (2015). Microbial community of the deep-sea brine Lake *Kryos* seawater-brine interface is active below the chaotropy limit of life as revealed by recovery of mRNA. *Environmental Microbiology*, 17(2), 364-382.  
<https://doi.org/10.1111/1462-2920.12587>

**Published in:**  
Environmental Microbiology

**Document Version:**  
Peer reviewed version

**Queen's University Belfast - Research Portal:**  
[Link to publication record in Queen's University Belfast Research Portal](#)

### **Publisher rights**

© 2014 Society for Applied Microbiology and John Wiley & Sons Ltd.

This is the accepted version of the following article: Microbial community of the deep-sea brine Lake Kryos seawater-brine interface is active below the chaotropy limit of life as revealed by recovery of mRNA, Michail M. Yakimov, Violetta La Cono, Gina La Spada, Giovanni Bortoluzzi, Enzo Messina, Francesco Smedile, Erika Arcadi, Mireno Borghini, Manuel Ferrer, Philippe Schmitt-Kopplin, Norbert Hertkorn, Jonathan A. Cray, John E. Hallsworth, Peter N. Golyshin and Laura Giuliano, which has been published in final form at <http://onlinelibrary.wiley.com/doi/10.1111/1462-2920.12587/abstract>.

### **General rights**

Copyright for the publications made accessible via the Queen's University Belfast Research Portal is retained by the author(s) and / or other copyright owners and it is a condition of accessing these publications that users recognise and abide by the legal requirements associated with these rights.

### **Take down policy**

The Research Portal is Queen's institutional repository that provides access to Queen's research output. Every effort has been made to ensure that content in the Research Portal does not infringe any person's rights, or applicable UK laws. If you discover content in the Research Portal that you believe breaches copyright or violates any law, please contact [openaccess@qub.ac.uk](mailto:openaccess@qub.ac.uk).

### **Open Access**

This research has been made openly available by Queen's academics and its Open Research team. We would love to hear how access to this research benefits you. – Share your feedback with us: <http://go.qub.ac.uk/oa-feedback>

1 Received date: 06/06/2014

2 Accepted date: 07/31/2014

3 Research Article for EMI Special Issue: *Microbiology of low water-activity habitats*. Subtopic:  
4 *Microbial diversity/community genomics of hypersaline systems*.

5 **Microbial community of the deep-sea brine Lake *Kryos* seawater-brine interface is**  
6 **active below the chaotropicity limit of life as revealed by recovery of mRNA.**

7 Michail M. Yakimov<sup>1,‡,\*</sup>, Violetta La Cono,<sup>1,‡</sup> Gina La Spada,<sup>1</sup> Giovanni Bortoluzzi,<sup>2</sup> Enzo Messina,<sup>1</sup>  
8 Francesco Smedile,<sup>1</sup> Erika Arcadi,<sup>1</sup> Mireno Borghini,<sup>3</sup> Manuel Ferrer,<sup>4</sup> Phillippe Schmitt-Kopplin,<sup>5,6</sup>  
9 Norbert Hertkorn,<sup>5</sup> Jonathan A. Cray,<sup>7</sup> John E. Hallsworth,<sup>7</sup> Peter N. Golyshin,<sup>8</sup> and Laura Giuliano,<sup>1,9</sup>

10

11 <sup>1</sup> *Institute for Coastal Marine Environment, CNR, Spianata S.Raineri 86, 98122 Messina, Italy.*

12 <sup>2</sup> *Institute for Marine Sciences, CNR, Via Gobetti 101, 40129 Bologna, Italy.*

13 <sup>3</sup> *Institute for Marine Sciences, CNR Forte S.Teresa, 19136 Pozzuolo di Lerici, La Spezia, Italy.*

14 <sup>4</sup> *Institute of Catalysis, CSIC, Marie Curie 2, 28049 Madrid, Spain.*

15 <sup>5</sup> *Analytical BioGeoChemistry, Helmholtz Zentrum München, German Research Center for Environmental*  
16 *Health, Neuherberg, Germany.*

17 <sup>6</sup> *Analytical Food Chemistry, Technische Universität München, Freising-Weihenstephan, Germany.*

18 <sup>7</sup> *Institute for Global Food Security, School of Biological Sciences, MBC, Queen's University Belfast, BT9 7BL,*  
19 *Northern Ireland.*

20 <sup>8</sup> *School of Biological Sciences, Bangor University, Bangor, Gwynedd LL57 2UW, UK.*

21 <sup>9</sup> *Mediterranean Science Commission (CIESM), 16 bd de Suisse, MC 98000, Monaco.*

22

23 \* Corresponding author

24 ‡ These authors contribute equally to this work.

25 *Running title:* Prokaryotes within the interface of deep-sea Lake *Kryos*

---

This article has been accepted for publication and undergone full peer review but has not been through the copyediting, typesetting, pagination and proofreading process, which may lead to differences between this version and the Version of Record. Please cite this article as doi: 10.1111/1462-2920.12587

1 *Key words:* Messinian evaporites, Deep-sea anoxic brine lakes, Halophiles, Limits of life,  
2 Chaotropy, Habitability, Mars

3

## Summary

Within the complex of deep, hypersaline anoxic lakes (DHALs) of the Mediterranean Ridge we identified a new, unexplored DHAL and named it "Lake *Kryos*" after a nearby depression. This lake is filled with  $\text{MgCl}_2$ -rich, athalassohaline brine (salinity >470 practical salinity units), presumably formed by the dissolution of Messinian bischofite. Compared to the DHAL *Discovery*, it contains elevated concentrations of kosmotropic sodium and sulfate ions, which are capable of reducing the net chaotropicity of  $\text{MgCl}_2$ -rich solutions. The brine of Lake *Kryos* may therefore be biologically permissive at  $\text{MgCl}_2$  concentrations previously considered incompatible with life. We characterized the microbiology of the seawater-*Kryos* brine interface and managed to recover mRNA from the 2.27-3.03 M  $\text{MgCl}_2$  layer (equivalent to 0.747-0.631 water-activity) thereby expanding the established chaotropicity window-for-life. The primary bacterial taxa present there were KB1 candidate division and DHAL-specific group of organisms, distantly related to *Desulfohalobium*. Two euryarchaeal candidate divisions MSBL1 and HC1, detected in minority in the overlaying layers, accounted for more than 85% of the rRNA-containing archaeal clones analyzed in 2.27-3.03 M  $\text{MgCl}_2$  layer. These findings shed light on the plausibility of life in highly chaotropic environments, geochemical windows for microbial extremophiles, and have implications for habitability elsewhere in the Solar System.

## Introduction

In the eastern part of Mediterranean seafloor, an accretionary complex, named the Mediterranean Ridge, is formed by subduction of the African plate under the Eurasian and Anatolian plates. During the Messinian salinity crisis (late Miocene epoch, 5.33 - 5.96 million years ago) the repeated desiccations and re-fillings of the Mediterranean Sea resulted in the formation of enormous deposits of layered evaporites, that attain the thickness of up to 3.5 km in some places of eastern Mediterranean (Cita, 2006). In contrast to other tectonically active ridges, the deformational activity of the Mediterranean Ridge accompanied with presence of huge subsurface salt deposits appears to control the creation of peculiar submarine hydrological formations within confined depressions. The peculiar hydrology and chemistry of such lakes, which are named deep-sea hypersaline anoxic lakes (DHALs), discourages mixing of their brines with the overlying seawater (Raup, 1970). Seven such lakes, L'Atalante, Bannock, Discovery, Medee, Thetis, Tyro and Urania have been discovered and studied in the deep eastern Mediterranean over the last 20 years (De Lange and Ten Haven, 1983; MEDRIF Consortium, 1995; Wallmann *et al.*, 1997; Chamot-Rooke *et al.*, 2005; La Cono *et al.*, 2011; Yakimov *et al.*, 2013). The surfaces of these brine lakes lie between 3.0 and 3.5 km below sea level and the salinity of their brines ranges from five to 13 times higher than that of seawater. Although these DHALs lie geographically close to each other (Fig. 1a), their hydrochemical diversity suggests that the processes leading to their formation were qualitatively different. As is generally accepted, during the desiccation/re-flooding cycles the salt deposition implied the simultaneous existence of early- and late-stage primary brines and evaporites. Seawater can be evaporated 10-fold without salt precipitation, resulting in formation of brine with salinity  $\leq 330$  PSU. This brine is named as "thalassohaline early-stage primary brine" (ESPB) and has proportions of all major ions characteristic to that of seawater. When the evaporation of seawater continues, salinity increases and the salts begin to precipitate changing the proportion of dissolved ions, thus forming the "athalassohaline late-stage primary brine" (LSPB). The insoluble calcium minerals precipitated first,

1 followed by precipitation of halite ( $\text{NaCl}$ ), kieserite ( $\text{MgSO}_4 \cdot \text{KCl} \cdot 3\text{H}_2\text{O}$ ), carnallite ( $\text{KMgCl}_3 \cdot \text{H}_2\text{O}$ ), kainite  
2 ( $\text{MgSO}_4 \cdot \text{KCl} \cdot 3\text{H}_2\text{O}$ ) and ending with formation of bischoffite ( $\text{MgCl}_2 \cdot 6\text{H}_2\text{O}$ ), which is the most soluble of  
3 all marine evaporite salts (Wallmann *et al.*, 1997; Cita, 2006). Due to favorable climatic and geological  
4 conditions, both brines and solid stratified evaporite suites were stored in the subsurface for  
5 millions of years until tectonic activities would squeeze them on the seabed. For some  
6 Mediterranean DHALs, their idiosyncratic geomorphology implies the formation mechanisms other  
7 than simple outcropping of the Messinian evaporites followed by accumulation of high-density  
8 brines in the nearby depression. As has been proposed elsewhere, the evaporite dissolution could  
9 occur in sub-bottom deposits without direct exposure on the seafloor (Camerlenghi, 1990;  
10 Camerlenghi and McCoy, 1990; Cita, 1991, 2006). Tectonic activity in the Mediterranean Ridge leads  
11 to tensional stress and formation of seabed fractures and through these seawater can penetrate into  
12 deeper sediment layers ultimately reaching the subsurface layer of the Messinian evaporites.  
13 Osmotic pressure encourages movement of seawater towards the solid evaporites, dissolving the  
14 most soluble salts and increasing the volume of internal brine lenses. Notably, this movement of  
15 seawater is almost unidirectional, because the argillaceous Plio-Quaternary superficial sediments  
16 overlying the Messinian evaporites are “salt-rejecting”, effectively behaving as a semipermeable  
17 membrane (Cita, 1991; 2006). Such continuing enrichment by evaporite dissolution leads to  
18 interstitial hydrologic formations, which in turn causes the overlying sediments to collapse and  
19 form a brine lake with characteristic confined, negative topography enriched by simple or complex  
20 morphologies ranging from sub-circular to elliptical, arc- or U-shaped basins, frequently including  
21 mounds and small, deeper depressions (Camerlenghi and McCoy, 1990).

22 Among all Mediterranean DHALs explored so far, only the *Discovery* Lake is filled with near-  
23 saturated  $\text{MgCl}_2$ -brine (5.05 M), suggesting that it derived via dissolution of bischofite, which is  
24 located within the uppermost layer of the evaporitic suite as explained above. Hence, the *Discovery*  
25 Lake is one of the saltiest athalassohaline water bodies on Earth (Table 1 and 2; Wallmann *et al.*,

1 1997, 2002). Due to the exceptionally high concentration of the divalent salt  $\text{MgCl}_2$ , this lake is  
2 approaching an anhydrous condition and is, simultaneously, an exceptionally chaotropic system  
3 with the lowest water activity ( $A_w$ ) value registered for any hydrological formation on our planet  
4 (Marion *et al.*, 2003; Hallsworth *et al.*, 2007). In our previous study we demonstrated that exceptional  
5 chaotropicity of  $\text{MgCl}_2$ , rather than water activity reduction, is the window-of-life-determining  
6 parameter (Hallsworth *et al.*, 2007). We suggested that in the absence of compensating (e.g.  
7 kosmotropic) ions, such as sodium and sulfates, the upper concentration of  $\text{MgCl}_2$ , permissible for  
8 life, is about 2.3 M. This finding is consistent with the apparent  $\text{MgCl}_2$  limit for microbial activity in  
9 the Dead Sea (Oren, 1999; 2010). As observed by Harrison *et al.* (2013), there have been relatively few  
10 studies on the way in which multiple stress parameters interact to determine the habitability of  
11 specific environments. A number of studies have, however, explored the way in which factors such  
12 as water activity, chaotropicity, nutrient availability and temperature can interact to determine  
13 biological permissivity of high-solute environments (Daffonchio *et al.*, 2006; Williams and  
14 Hallsworth, 2009; Chin *et al.*, 2010; Cray *et al.*, 2013a; 2013b; Lievens *et al.*, 2014).

15 Here, we present the results of the first oceanographic, geochemical and microbiological  
16 explorations of Lake *Kryos*, a second Mediterranean athalassohaline DHAL filled with nearly  
17 saturated  $\text{MgCl}_2$ -brine. Aside from slightly elevated concentrations of  $\text{Na}^+$  and  $\text{SO}_4^{2-}$ , the  
18 hydrochemistry of this novel lake was found to share commonalities with that of the Lake *Discovery*  
19 (Table 1). As revealed by a comprehensive analysis of the vertical distribution of major prokaryotic  
20 groups along the seawater-brine interface, the *Kryos* prokaryotic community forms sharply  
21 stratified and dense ecosystem, operating at the very edge of Earth's biosphere. In order to decipher  
22 the stratification of principal metabolic pathways within this environment and, considering that  
23 DNA may be effectively conserved under highly chaotropic conditions, comparative analysis of  
24 recovered rRNA and mRNA transcripts were performed for three layers of the interface.

25

## 1 Results and discussion

### 3 *Geomorphological and geochemical characterization of Lake Kryos.*

5 During the cruise MIDDLE08 on RV *Urania* in September 2008, while on transit from the *Anoxic*  
6 *Lakes Region* West of Crete to the Lake *Medee*, we surveyed by 3.5 Chirp kHz swath-bathymetry  
7 profiling (SBP) confined depressions deeper than or similar to known seawater : DHAL interfaces  
8 (Fig. 1a). The candidate targets were localized by the morpho-bathymetric analysis of MEDIMAP data  
9 with resolution of 500 m (Loubrieu *et al.*, 2008). Given that the strong density contrast at the  
10 seawater-brine lake interface would have produced a straight line on acoustic swath bathymetrical  
11 profiling (SBP) data, we expected to be able to identify some yet unexplored DHALs. Approximately  
12 20 nautical miles from the *Urania* Lake, we moved over a narrow North-South, elongated fracture  
13 ( $22^{\circ}01'E$   $35^{\circ}02'N$  –  $22^{\circ}02'E$   $34^{\circ}53'N$ ) and a sharp crisp line, hinting at the existence of a brine lake, was  
14 detected with maximum depth of about 3500 m. This was confirmed by direct conductivity-  
15 temperature-dissolved oxygen (CTD) profiling, brine sampling and bottom coring. Using the SBP  
16 data of the RV *Urania* DEEPPRESSURE cruise in 2013 and correcting the depths in the brines with the  
17 pressure data of the CTD casts, we obtained a map of the *Kryos* Lake with 20 to 25 m resolution. The  
18 Lake *Kryos* (named after the neighboring oxic depression) has the seawater-brine interface at 3387  
19 dB (3337 m) and fills a steep, narrow basin approximately 18 km long and 1.7 km wide, oriented N-S  
20 and bending N-N-E at its northern tip with two arms oriented E-N-E (Fig. 1b). The bottom of the  
21 basin is 300-400 m below the depth of the surrounding region and has a well defined, continuous and  
22 very steep slope to the west, while in the opposite direction the seabed rises more moderately. The  
23 southern part of *Kryos* basin is characterized by several N-S oriented mounds and depressions,

1 presumably indicating the existence of isolated brine pools. Similar small pools may be detected at  
2 the northernmost part of the lake. Lake *Kryos*, including these small polar pools, has an area of  
3 about 100 km<sup>2</sup> and a volume of about 10 km<sup>3</sup>. The central area of the lake is slightly deeper than 3500  
4 m below sea level, implying that the depth of brine within the lake is approximately 160-170 m. The  
5 temperature measured at the seawater : brine interface was 13.98°C and slightly increased to 14.66°C  
6 within the brine, close to the seabed.

7 Chemical characterization of the *Kryos* brine revealed its extremely high salinity (471 g [kg  
8 H<sub>2</sub>O]<sup>-1</sup>) mainly due to extreme, close to saturation, concentration of Mg<sup>2+</sup> (4.38 M) and Cl<sup>-</sup> (9.04 M). As  
9 shown in the Table 1, the *Kryos* hydrochemistry is quiet similar to that of the *Discovery* brine with  
10 the exception of elevated concentrations of Na<sup>+</sup> and SO<sub>4</sub><sup>2-</sup>, which are present in the former. The  
11 *Kryos* basin is filled with almost 10 km<sup>3</sup> of MgCl<sub>2</sub>-rich brine which compares to Lake *Discovery*  
12 volume of nearly 0.2 km<sup>3</sup> (Wallmann *et al.*, 1997, 2002); the DHAL *Kryos* is thus the largest deep-sea  
13 athalassohaline formation on Earth. Moreover, Lake *Discovery*, the CaCl<sub>2</sub>-saturated *Don Juan Pond*  
14 and Lake *Kryos* together form a triad of the saltiest aquatic systems on our planet (Table 2).  
15 Previously made equilibrium calculations with the PHRQPITZ model (Wallmann *et al.*, 1997) have  
16 indicated that a LSPB similar in composition to those of the MgCl<sub>2</sub>-rich athalassohaline brines may  
17 be produced when seawater is evaporated to the point of bischoffite precipitation, i.e. until only 5 g  
18 of initial 1000 g of H<sub>2</sub>O remained in solution. A similar composition, termed as a secondary brine  
19 (SB), may also be formed when seawater is equilibrated with solid bischoffite and kainite  
20 (K<sub>4</sub>Mg<sub>4</sub>Cl<sub>4</sub>(SO<sub>4</sub>)<sub>4</sub>·11H<sub>2</sub>O) (Table 2). Therefore, the major ion composition of both brine lakes is  
21 consistent with either a primary (evaporated seawater) or secondary origin (dissolution of the most  
22 soluble marine evaporite salts). As it generally accepted, concentrations of lithium could be used to  
23 differentiate between the primary and secondary brines, because this cation is conserved during  
24 seawater evaporation path and does not co-precipitate with evaporites in the presence of high Mg<sup>2+</sup>  
25 concentrations (Carpenter, 1978; McCaffrey *et al.*, 1987; De Lange *et al.*, 1990; Wallmann *et al.*, 1997,

2002). By comparison with the LSPB values, lithium concentration in the *Discovery* and *Kryos* brines was 20-25 times less, indicating that both lakes have evidenced an extreme evaporation of the eastern Mediterranean, which is likely to have taken place during the late Messinian. As was proposed for Lake *Discovery*, the upmost layer of evaporite suite, represented by precipitated and lithium depleted bischoffite, was subsequently re-dissolved and has migrated to form a deep-sea brine pool. As it was shown by analysis of  $^4\text{He}$  concentrations, before it entered the *Discovery* basin, the re-dissolved  $\text{MgCl}_2$ -saturated brine was initially stored for unknown period of time inside the sediments as interstitial brine pool (Wallmann *et al.*, 1997, 2002). We hypothesized that this scenario of the origin is equally applicable to the *Kryos* Lake.

#### *The Kryos and Discovery Lakes are the most chaotropic large-scale aquatic systems on Earth*

Earlier we have measured the water activities ( $A_w$ ) in various  $\text{MgCl}_2$ -dominated solutions and evidenced that this salt is one of the most powerful  $A_w$ -reducing agents known (Hallsworth *et al.*, 2007); see also Winston and Bates (1960). Due to its high solubility and divalency,  $\text{MgCl}_2$  is able to depress the water-activity values much below the limit observed for cell division or metabolic activity (Fig. 2a; Pitt, 1975; Marion *et al.*, 2003; Grant, 2004; Williams and Hallsworth, 2009). The water activity of saturated  $\text{MgCl}_2$  is 0.340 in the range 10 - 15°C (Fig. 2a; Winston and Bates, 1960); we empirically determined the value for the *Discovery* brine; which was 0.382  $A_w$  at 14.5°C (Hallsworth *et al.*, 2007). However, the established water-activity limit for (active) life (0.605<sup>2</sup>; Pitt and Christian, 1968) is equivalent to 3.7 M  $\text{MgCl}_2$  (Hallsworth *et al.*, 2003a, 2007). The brine of *Kryos* contains a considerably higher concentration of  $\text{MgCl}_2$  (4.38 M), which corresponds to 0.399  $A_w$ . Another

---

<sup>2</sup> Whereas there have been a number of unsubstantiated claims of germination and growth of *Streptomyces* and *Micromonospora* strains at 0.500  $A_w$  from one research group (Doroshenko *et al.*, 2005; 2006; Zvyagintsev *et al.*, 2007; 2009; 2012; Kurapova *et al.*, 2012), the limit for such Actinobacteria has recently been determined empirically at 0.890  $A_w$ , with a theoretical lower limit which was derived by construction of isopleths growth profiles of approximately 0.870  $A_w$  (Stevenson and Hallsworth, 2014).

1 harmful feature of  $\text{MgCl}_2$ -rich solutions, incompatible with existence of actively metabolizing  
2 organisms, is their exceptional chaotropicity (Hallsworth *et al.*, 2007; Cray *et al.*, 2013a), and it is this  
3 property, rather than any other activity of the solute, which can limit the microbial biosphere in  
4 high- $\text{MgCl}_2$  (and presumably other highly chaotropic) environments (Hallsworth *et al.*, 2007).  
5 Supporting this, our previous study on microbial communities of the *Discovery* Lake and recovery of  
6 unstable biomarkers, such as messenger RNA, suggested that in almost pure solutions of  $\text{MgCl}_2$   
7 representing the *Discovery* brine, the active life, as we currently know it, is not likely at  $\text{MgCl}_2$   
8 concentrations of  $> 2.3 \text{ M}$  (Hallsworth *et al.*, 2007), which corresponds to  $< 0.790 A_w$  (Fig.2a). We are  
9 aware that the equation between these specific chaotropicity and water-activity values might be  
10 true only for the *Discovery* brine, almost depleted by sodium and sulfates. However, various sources  
11 of evidence suggest that this limit can also be expected for other habitats because chaotropes can to  
12 some extent be compensated by kosmotropes (Oren, 1983; Hallsworth *et al.*, 2003b, 2007; Williams  
13 and Hallsworth, 2009; Bhaganna *et al.*, 2010; Bell *et al.*, 2013), so the presence of other anions, like  
14 sodium and sulfate, can reduce the net chaotropicity of a hypersaline environment and widen the  
15 chaotropicity windows of life. Compared with the Lake *Discovery*, the Lake *Kryos* brine is slightly  
16 impoverished with  $\text{MgCl}_2$  and simultaneously enriched with kosmotropic sodium and sulfate ions  
17 (Table 1), thus representing a unique opportunity to explore and test this assumption.

18 As shown in Figure 3, there is a sharp,  $\sim 2.5 \text{ m}$  halocline at the seawater : brine lake interface  
19 characterized by a steep  $\text{Mg}^{2+}$  gradient ranging in concentration from  $55 \text{ mM}$  at its upper layer to  
20  $4.38 \text{ M}$  in proximity to brine. Using our previous approach for  $A_w$  measurements of  $\text{MgCl}_2$  solutions  
21 applied to *Discovery* samples (Hallsworth *et al.*, 2003b; 2007), we measured the  $A_w$  and chaotropicity  
22 levels of the *Kryos* interface (Fig. 2). The current window for chaotropicity equivalent ( $A_w = 0.790$ ),  
23 established for the interface of *Discovery*, and the current window for xerophilic cellular life  
24 ( $A_w=0.605$ ) embrace only upper two-thirds of the *Kryos* interface. An  $A_w$  value of  $0.399$  was  
25 determined for the *Kryos* brine itself and it is far below a minimal level of water activity, essential

for cellular function. The *Kryos* brine is thus an exceptionally chaotropic and low-water-activity environment, possibly the most large-scale,  $\text{MgCl}_2$ -saturated, aquatic system on Earth.

One year after the discovery of Lake *Kryos*, we begun exploring the extent to which cellular systems have been able to adapt to the *Kryos* interface conditions. Following this aim, the *Kryos* interface was sampled and fractionated using our previously established methodology to sample the DHAL interfaces (Daffonchio *et al.*, 2006; Borin *et al.*, 2009; Hallsworth *et al.*, 2007; Yakimov *et al.*, 2007a, 2007b, 2013; La Cono *et al.* 2011). Immediately after the rosette recovery, initial measurements of salinities of the bottommost content of Niskin bottles were performed. Obtained values were plotted over the reconstructed salinity profile (Fig. S1). We were aware that accurate capturing from elevated depths of *in situ* patterns of extremely unstable mRNA is potentially biased by changes in environmental conditions during the sample recovery (Feike *et al.*, 2012). To diminish this concern, all interface layers carrying similar biases, were sampled during the same cast and were processed in parallel. Due to the favorable weather conditions, little or no mixing had occurred during the sampling. Five Niskin bottles, exhibiting equivalent salinities at their bottoms, were used for further biological analyses (Fig. S1). Their contents were carefully fractionated anaerobically by slowly recovering 0.5-litre, 1-litre or 2-litre fractions from bottom tap. The subsamples collected from the bottommost part of these Niskin bottles (range of  $\text{MgCl}_2$  2.27 - 3.03 M) were pooled and hereafter termed as the AWW layer. As shown in Fig. 2a, the calculated  $A_w$  values for this layer (from 0.747 to 0.631) extend beyond both the established chaotropicity limit for life<sup>3</sup> and close to the established water-activity limit for cell division of prokaryotes (for references, see Grant, 2004; Stevenson *et al.*, 2014). As anticipated, the presence of kosmotropic substances in the *Kryos* brine, such as sulfates, has a mitigating effect on the chaotropicity of  $\text{MgCl}_2$  (Fig. 2b). For example, at ~0.760  $A_w$  agar-gel point temperatures for both the *Kryos* brine and synthetic *Kryos* brine were ~6°C

---

<sup>3</sup> Based on the chaotropicity -  $A_w$  equivalence for the closest comparator brine, that of the *Discovery* lake (Hallsworth *et al.*, 2007).

1 higher than that of a  $\text{MgCl}_2$  solution (Fig. 2b). This temperature difference is equivalent to a  
2 kosmotropicity of  $25 \text{ kJ kg}^{-1}$  (Hallsworth *et al.*, 2013a; Cray *et al.*, 2013a); the kosmotropic activity  
3 that is exerted by 2.3 M NaCl (Hallsworth *et al.*, 2007). The overlaying layer, hereafter termed CHW,  
4 had the range of  $\text{MgCl}_2$  concentrations 1.30 – 2.27 M, corresponding to the established chaotropicity  
5 boundary (CHW) (Fig. S1), so the *Kryos* brine potentially represents habitable high- $\text{MgCl}_2$   
6 environment thus far identified; equivalent to a chaotropicity of between 143 and  $296 \text{ kJ kg}^{-1}$  (Fig.  
7 S2). The upper interface (UIF) layer with salinity of 50-140 PSU was additionally analyzed to affirm  
8 the occurrence of stratified and metabolically active microbial populations thriving in deeper AWW  
9 and CHW compartments.

#### 11 *Characterization of dissolved organic matter in the Kryos brine*

13 After dissolved organic matter (DOM) isolation by means of solid phase extraction, the desalted  
14 eluate was analyzed with ultrahigh resolution mass spectrometry (ion cyclotron resonance  
15 Fourier transform mass spectrometry, ICR-FT/MS) enabling a direct depiction of the DOM  
16 compositional space with a few thousands of assigned elemental formulas of this complex organic  
17 mixture. The mass spectra show a near Gaussian signal distribution typical of natural organic  
18 matter, with recognizable main mass spacings of methylene ( $\Delta m = 14.056 \text{ amu}$ ), double bond  
19 equivalents (DBE,  $\Delta m = 2.0157 \text{ amu}$ ) and a splitting of  $\Delta m = 0.0024 \text{ amu}$ , denoting closely spaced  
20 CHO and CHOS compounds (Schmitt-Kopplin *et al.*, 2010a) indicative of a highly processed  
21 organic matter with appreciable extent of sulfurization at a relatively small overall molecular  
22 weight ( $<500 \text{ amu}$ , Fig. 4a). Conversion of the signals into elemental compositions revealed a high  
23 abundance of sulfur compounds (700 CHOS and 250 CHNOS were assigned molecular formulas)  
24 reflecting the remarkable diverse sulfur chemistry in these particular extreme sulfide rich

1 environments (Fig. 4b,c). Neither organochlorines nor organomagnesium compounds were  
2 indicated by these datasets. The ratios of CHOS/CHO and CHNOS/CHNO molecular compositions  
3 in DOM were different, reflecting divergent mechanisms of sulfurization resulting in CHOS and  
4 CHNOS molecules. In contrast, purely abiotic reactivity of reactive sulfur species of presumably  
5 mineral origin with CHO and CHNO compounds led to comparable ratios (Schmitt-Kopplin *et al.*,  
6 2010b). Hence, a biotic origin of the sulfur compounds observed in the *Kryos* brine seems highly  
7 likely. The van Krevelen diagrams show compounds with rather pronounced aliphaticity  
8 (elevated H/C ratio) and especially remarkable extent of oxygenation (O/C ratio > 0.6), extending  
9 even further than the previously described carboxyl-rich alicyclic materials (CRAM) (Fig. 4d).  
10 Further research is needed to elucidate the structural diversity of these compounds resembling  
11 the condensed alicyclic structures of biogenic origin such as sterols and hopanoids, which offer  
12 nominal unsaturation without overly abundance of sp<sup>2</sup> carbon (Hertkorn *et al.*, 2006).

#### 14 *Prokaryotic abundance and community composition of the Kryos interface using CARD-FISH*

15  
16 At the depth of ~3338 m, where the UIF *Kryos* sample was taken, total prokaryote number (DAPI-  
17 stained cells) increased six-fold compared to DAPI values for overlaying deep-sea water (Table 3).  
18 The number of cells in the CHW interface layer increased to  $5.57 \pm 0.45 \times 10^5$  cell ml<sup>-1</sup> and then  
19 gradually decreased to  $2.47 \pm 0.11 \times 10^5$  cell ml<sup>-1</sup> in the AWW layer, which was below the CHW. CARD-  
20 FISH indicated that while almost all DAPI-stained cells from the overlaying seawater contained 16S  
21 rRNA (89%), the numbers of CARD-positive microorganisms in the UIF interface layer dropped  
22 almost to a half of those visualized by DAPI (53 %). The gradual increase of CARD-positive fraction  
23 from 68 to 81% of all DAPI-stained cells was observed in deeper layers (Table 3). This phenomenon of  
24 increase in cell density likely reflects trapping and effective conservation under highly chaotropic  
25 conditions of stable biological macromolecules, such as DNA and rRNA, albeit in an inactivated form

(Duda *et al.*, 2004; Hallsworth *et al.*, 2007; Cray *et al.*, 2013a). Nevertheless, the existence of as-yet-undiscovered life forms, that have evolved greater chaotropicity and water activity tolerances than presently known, cannot be ruled out (Hallsworth *et al.*, 2007).

As revealed by taxon-specific CARD-FISH analysis (Table 3 and Table S1), bacteria dominated all studied layers of the *Kryos* interface. Previously we have shown that bacterial community thriving in the low interface of Lake *Discovery* was characterized by overwhelming dominance of members of KB1 candidate division and organisms, distantly related to *Desulfohalobium* (Hallsworth *et al.*, 2007). Application of KB1-specific FISH-probes (Yakimov *et al.*, 2013) revealed that, being absent in UIF community these extremely halophilic prokaryotes are gradually dominating the CHW and AWW populations. Distribution of DHAL-specific deltaproteobacteria was found be more homogeneous in both saltiest layers. Thaumarchaeota and Euryarchaeota exhibited opposing distribution patterns in relation to depth. The absolute dominance of Euryarchaeota in hypersaline and anoxic habitats is a characteristic feature for all currently studied DHALs interfaces (Daffonchio *et al.*, 2006; Borin *et al.*, 2009; Hallsworth *et al.*, 2007; Yakimov *et al.*, 2007a, 2007b, 2013; La Cono *et al.*, 2011). Noteworthy, below the established  $A_w$ -limit of life (0.605) the CARD-FISH analysis with the universal archaeal probe ARCH915 detected more than 40000 ribosome-containing cells  $ml^{-1}$ , whereas none of them were visualized there by more specific EURY806 probe (Table 3). This observation can be explained by the presence in the AWW samples of organisms, such as the members of MSBL1 candidate division, whose 16S rRNA sequences are out of the EURY806 probe specificity range.

*Stratification of the Kryos interface prokaryotic 16S rRNAs across the chaotropicity limit of life*

1 To survey the distribution of ribosome-containing Bacteria and Archaea, total RNA (50.42, 35.37  
2 and 32.18 ng  $\mu\text{l}^{-1}$ ) was respectively extracted from UIF, CHW and AWW samples. Total cDNA was  
3 further obtained by reverse transcription with hexa-random primers, PCR amplified with 16S  
4 rDNA-specific primers (Table S2), cloned and a total of 464 and 386 archaeal and bacterial inserts  
5 were partially sequenced. Phylogenetic analysis of the resulting reads revealed a pronounced  
6 stratification of prokaryotes thriving in the extremely chaotropic and salty compartments of the  
7 *Kryos* interface just above and below the established chaotropy boundary of life (Fig. 5a).  
8 Remarkably, presence of layer-specific groups of 16S rRNA sequences in all three samples  
9 indicated that accurate fractionation of the *Kryos* interface was successful and reciprocal mixing  
10 had not occurred during recovery and subsequent processing of gradient samples. As for the  
11 overlaying deep seawater, members of Marine Group I Thaumarchaeota dominate the UIF  
12 archaeal community. In concordance with CARD-FISH analysis, ribosomal RNA-containing  
13 dormant thaumarchaeal cells have been settled in deeper interface compartment CHW from  
14 above layers, thus resulting in a significantly distorted indication of diversity of autochthonous  
15 metabolically active archaeal population. Two groups of halophilic Euryarchaeota, the MSBL1 and  
16 HC1 candidate divisions, detected in minority in the CHW layer, became dominant euryarchaeal  
17 groups in AWW layer, accounting for more than 85% of all archaeal clones (Fig. 5b). 16S rRNA  
18 sequences of extremely halophilic haloarchaea and methylotrophic methanogens, also being  
19 presented in CHW by singletons, were remainders of the AWW archaeal community. Remarkably,  
20 together with clones retrieved from the Lake *Discovery*, the MSBL1- and Halobacteriales-related  
21 *Kryos* clones formed separate clusters, which constitute evidence for the existence of  $\text{MgCl}_2$ -  
22 adapted species or genera within these candidate divisions (Fig. 6).

23 The empirically determined water-activity value for the 3.03 M  $\text{MgCl}_2$  *Kryos* layer is 0.631,  
24 which is considerably close to the established limit for growth of halophilic prokaryotes (i.e.

1 ~0.755; Grant, 2004). Recent studies, however, have demonstrated cell division of more than 10  
2 halophilic prokaryotes, including members of the Halobacteriales in the range 0.717 to 0.6011  $A_w$   
3 (JE Hallsworth *et al.*, unpublished data) and the findings of the current study are consistent with  
4 their water-activity minima. These include empirically determined  $A_w$  values of 0.693 for  
5 *Halococcus salifodinae*, 0.687 for *Halobacterium noricense*, and 0.681 for *Natrinema pallidum* as  
6 well as values derived by extrapolation of 0.680 for *Halorhodospira halochloris*, 0.675-0.670 for  
7 halophilic bacteria belonging to the *Salinibacter* assemblage from crystallizer pond CR-30 (Braç  
8 del Port, Alicante), 0.668 for *Haloanaerobium lacusrosei*, 0.660 for *Actinopolyspora halophila*,  
9 0.658 for *Halobacterium* strain 004.1, 0.647 for *Halorhabdus utahensis*, 0.623 for *Halorhodospira*  
10 *halophila*, 0.615 for *Halobacterium* strain GN-5, and 0.611 for *Halobacterium* strain GN-2.

11 Phylogenetic composition of the bacterial fraction recovered from all three analyzed  
12 layers is shown in Figure 5a and in Supplementary Material (Figure S3 and S4). Compared with  
13 the UIF and CHW 16S rRNA libraries, much lower diversity of bacterial phylotypes was recovered  
14 from the AWW layer of the *Kryos* interface. This included members of KB1 candidate division  
15 (54% of all clones sequenced) and yet unknown hyperhalophilic groups of the class  
16 Deltaproteobacteria (rest of the AWW clones) (Fig. 5b). Whereas coherent KB1-related organisms  
17 thrived also in the upper CHW layer, two phylogenetic clusters of Deltaproteobacteria, probably  
18 representing different extremely halophilic genera, were detected exclusively in the ultimate  
19 layer of the water-activity window for life (AWW) (Fig. 7). The less chaotropic and less salty CHW  
20 layer of the *Kryos* interface was inhabited by completely distinct population of  
21 Deltaproteobacteria, consisting of sulfate reducing bacteria (SRB) distantly related to the genera  
22 *Desulfotignum* and halophilic *Desulfosalsimonas* (Fig. 7). Noteworthy, all bacterial AWW  
23 phylogenetic groups have close relatives recovered from sediments of the Mediterranean solar  
24 salterns and surficial hypersaline lakes *Aran-Bidgol* (Iran) and *Tebenquiche* (Chile) (Demergasso

1 *et al.*, 2008; Baati *et al.*, 2010; Makhdoumi-Kakhki *et al.*, 2012), thus considerably reducing the  
2 sampling efforts needed for their eventual culturing and the study of their physiology and  
3 metabolism.

4 As we have shown previously (Hallsworth *et al.*, 2007), bacterioplankton from overlaying  
5 compartments once entered by sedimentation in the sterile *Discovery* brine, is accumulating  
6 there at such highly conserved state that DNA from these organisms can be amplified.  
7 Consequently, DNA-based methodologies seem inaccurate approaches to study the “signatures of  
8 active life” under highly chaotropic conditions. Indeed, phylogenetic analysis of total DNA  
9 sampled at the depth of 3370 m revealed the occurrence in the *Kryos* brine of 16S rDNA  
10 signatures belonging to both Bacteria and Archaea dominating the deep-sea seawater and  
11 surficial layers of the interface, but missing in AWW layer (Figures 5a and S3-S5). Namely, almost  
12 30% and 15% of all bacterial and archaeal clones recovered from the *Kryos* brine were  
13 respectively attributed to the Epsilonbacteria and Marine Group I Thaumarchaeota, the groups of  
14 prokaryotic organisms which dominated the UIF and CHW layers but were undetectable in the  
15 AWW layer. Similar distribution patterns, i.e. lack in AWW but occurrence in the *Kryos* brine,  
16 were observed for the members of Bacteroidetes, Gammaproteobacteria, Planctomycetes and  
17 archaeal candidate division SA1. None of brine-specific archaeal 16S rRNA sequences different  
18 from that of UIF, CHW and AWW libraries was detected in the *Kryos* brine, suggesting that all  
19 prokaryotic diversity detected in the *Kryos* brine derived from the overlaying deep seawater  
20 column and the interface. UniFrac PCA analysis affirmed that the microbial community of the  
21 *Kryos* interface exhibited notable stratification, mediated by a succession of different groups of  
22 organisms. Whereas being marginally different from the intermediate CHW layer ( $P = 0.039$ ), the  
23 AWW bacterial population resulted statistically different from the less salty UIF sample ( $P < 0.001$ )  
24 (Fig. S6a). Consistently with the statement that the *Kryos* brine acts as a trap for descending  
25 allochthonous bacterioplankton, no statistical significant distance was found between BB (DNA-

based survey) and AWW layers; and only small difference was observed between BB and CHW layers ( $P = 0.033$ ). The archaeal community behaved in similar manner, although the detected stratification was found to be less pronounced due to aforementioned influence of Marine Group I Thaumarchaeota. Both statistically allied AWW and BB layers resulted only slightly different from the UIF sample (corresponding  $P$  values of 0.12 and 0.18) and no statistical significant distances between the AWW, BB and CHW layers were detected (Fig. S6b).

*Evidence that metabolic activity occurs in the AWW layer; i.e. below the established chaotropicity window for life*

As mentioned above, the majority of the AWW archaeal community comprised of the MSBL1 and HC1 candidate divisions. Previously we speculated, that on basis of phylogenetic relatedness to methanogens and the lack of other groups that might be responsible of the detected methane production in some of Mediterranean DHALs, the MSBL1 members might be involved in methanogenesis at high salinity (van der Wielen *et al.*, 2005; Daffonchio *et al.*, 2006; Borin *et al.*, 2009; Yakimov *et al.*, 2013). Due to the fact that genetic determinants for methanogenesis in MSBL1 organisms remain unknown, we cannot examine their metabolic activities. Nevertheless, the phylogenetic lineage related to the genus *Methanohalophilus* was detected in AWW interface layer as considerable fraction of clones (5%), thus making feasible the assessment of their methanogenic activity via the recovery of alpha subunit of methylcoenzyme M reductase (*mcrA*) gene transcript. Unlike the *mcrA* diversity of the *Discovery* interface, where only *Methanohalophilus*-related sequences were detected (Hallsworth *et al.*, 2007), the *Kryos* interface possessed two distinct phylogenetic clusters of this gene (Fig. 5a). The CHW-specific *mcrA* group was found be distantly related to methylcoenzyme M reductase of *Methanomassiliicoccus*

1 *luminyensis*. This methylotrophic methanogenic *Thermoplasma* archaeon carries a reduced  
2 methanogenesis pathway, restricted by reduction in the presence of H<sub>2</sub> of methanol and other  
3 methylated compounds to methane (Dridi *et al.*, 2012; Grolas *et al.*, 2012; Borrel *et al.*, 2013).  
4 Although this type of metabolism was never sought in the DHAL ecosystems, the eventual  
5 occurrence of this obligate H<sub>2</sub>-dependent methylotrophic type of methanogenesis should be  
6 taken into account in future studies and cultivation attempts. Coherently with the *Discovery*  
7 *mcrA* gene expression survey, the diversity of the AWW *mcrA* transcripts was extremely low and  
8 all sequences were found be almost identical to that retrieved from the deepest, populated layer  
9 of the *Discovery* interface (2.23 M of MgCl<sub>2</sub>) (Hallsworth *et al.*, 2007). This observation confirmed  
10 the assumption that the AWW layer of the *Kryos* interface is inhabited by a distinct archaeal  
11 population, which is able to thrive at high concentrations of Mg<sup>2+</sup>.

12 The bacterial community of the AWW layer characterized by an extremely low diversity,  
13 with only two major taxa of hyperhalophilic organisms present. Similarly to MSBL1, lack of  
14 genomic information of the KB1 candidate division precludes any of metabolic gene expression  
15 surveys. However, the metabolic activity of sulfur reducing deltaproteobacteria in the AWW layer  
16 of the *Kryos* interface was indicated by the recovery and analysis of *dsrAB* gene transcripts. It is  
17 important to note that the AWW layer contained both the highest H<sub>2</sub>S concentration and the  
18 number of SRBs-related sequences in all three layers analyzed, pointing out to an important  
19 ecological role of their members in the sulfur cycle of the *Kryos* ecosystem. This statement is also  
20 coherent with the analysis of DOM in the sterile *Kryos* brine, where the biotic sulfur compounds,  
21 obviously originated from the overlaying interface, were observed. The existence of hitherto  
22 unknown hyperhalophilic groups within SRBs was subsequently corroborated by the  
23 phylogenetic attribution of *dsrAB* gene transcripts recovered from the AWW layer (Fig. 7).  
24 Remarkably, the recovery and further analysis of *dsrAB* gene transcripts revealed the presence in  
25 the AWW layer of the sequences distantly related to that of *Desulfotignum balticum* and

1 halophilic *Desulfosalsimonas propionica*. This observation let us to an assumption, that once  
2 immersed in the AWW layer, these organisms can likely withstand the high concentrations of  
3  $Mg^{2+}$  and remain, albeit briefly, metabolically active.

#### 5 *Concluding remarks*

6  
7 The results obtained in this study portray a very stratified indigenous prokaryotic community  
8 thriving at the edge of life in the  $MgCl_2$ -rich DHAL *Kryos* interface under highly chaotropic  
9 conditions. The 25-cm thick *Kryos* interface layer AWW was sampled in range from 2.27 to 3.03 M of  
10  $MgCl_2$ , which corresponds to salinity of 245 – 330 PSU and water activity values from 0.747 to 0.631.  
11 Despite lying beyond the established chaotropicity and prokaryotic life boundaries, the AWW layer  
12 seems inhabited by a highly specific community of prokaryotes far different from the thriving above  
13 communities. The majority of our AWW archaeal clones (85%) were affiliated to the candidate  
14 divisions MSBL1 and HC1 that branched deeply within the Euryarchaeota. These divisions were  
15 proposed recently to comprise the majority of the archaeal clones retrieved from the deep-sea  
16 Mediterranean Sea Brine Lakes (MSBL) and surficial salt-saturated anoxic lakes (van der Wielen *et al.*,  
17 2005; Jiang *et al.*, 2007). The divisions are equivalent in genetic depth and breadth to  
18 Halobacteriales and likely represent new orders of yet-to-be-cultivated taxa (van der Wielen *et al.*,  
19 2005). The haloarchaeal *Kryos* AWW clones together with the clones retrieved from the Lake  
20 *Discovery* formed a distinct, deeply branched cluster within Halobacteriales, thus eventually  
21 inferring the existence of new,  $MgCl_2$ -adapted species or genera. Similarly to archaeal community,  
22 the AWW bacterial phylotypes belonged to hitherto uncultured hyperhalophilic organisms, present  
23 exclusively in the DHALs and in highly reduced sediments of some surficial hypersaline lakes

1 habitats. Noteworthy, the *Kryos* microbial community, thriving below the established chaotropicity  
2 boundary for life, previously established for the Lake *Discovery*, was found be very similar, at least at  
3 the level of 16S rRNA phylogeny, to that of the other most hypersaline anoxic environments  
4 sampled worldwide. It is plausible that obligate anaerobic hyperhalophiles, adapted to thrive in salt-  
5 saturated habitats under low- $A_w$  conditions, possess hitherto uncharacterized mechanisms to resist  
6 chaotropicity and to be metabolically active in such harsh athallasohaline habitats (e.g. exceptional  
7 levels of cellular desiccation, or unusual and/or highly kosmotropic compatible solutes; Potts, 1994;  
8 Cray *et al.*, 2013a; Wyatt *et al.*, 2014a; 2014b). The relevance of our findings encourages digging into  
9 the genetic and metabolic diversity of these  $MgCl_2$ -adapted hyperhalophiles. We are, therefore,  
10 conducting additional culturing and metagenomic approaches to obtain a better understanding of  
11 the functioning of the *Kryos*-interface ecosystem.

12 Thus, at present, we must conclude that the question of the window of tolerance of life (i.e.  
13 cellular division and/or metabolic activity) for chaotropic activity remains yet open. Compared to  
14 Lake *Discovery*, the *Kryos* lake contains slightly elevated concentrations of the kosmotropic ions  $Na^+$   
15 and  $SO_4^{2-}$ . These ions, via their compensating effect against extreme chaotropicity of  $MgCl_2$  solutions,  
16 are likely to enable cellular activities at  $MgCl_2$  concentrations which hitherto considered  
17 incompatible with life (Hallsworth *et al.*, 2007). In concordance with our previous statement, we may  
18 conclude that life in environments with extremely high concentrations of  $MgCl_2$  is unlikely.  
19 Nevertheless, the simultaneous presence of kosmotropic ions in Mg-rich environments decreases  
20 their chaotropicity and thus, turns them inhabitable for diverse hyperhalophilic microbes. This  
21 assumption also has implications for hypersaline Mg-rich milieu, which are known to be located in  
22 extraterrestrial environments. However, chaotropic substances such as  $MgCl_2$  can be beneficial at  
23 low temperatures (those below 10°C, and most especially sub-zero temperatures) by enhancing the  
24 flexibility of macromolecule systems, which permits cellular function and thereby reduces the

temperature minimum for cell division of psychrotolerant or psychrophilic microbes (Chin *et al.*, 2010). Ironically, therefore, the possibility remains that high concentrations of  $\text{MgCl}_2$  (or other chaotropic salts) on moons or other planetary bodies, which are colder than Earth may potentially increase habitability of aqueous milieu.

## Experimental procedures

### *Oceanographic and geophysical characterization of Kryos basin*

The morphobathymetric analysis of the Mediterranean Sea at 500 m resolution (Loubriueu *et al.*, 2008) was used to locate confined depressions deeper or equal than known DHALs interfaces depths (on average 3200-3300m). The target areas were therefore investigated with the RV *Urania* hull mounted 16 transducer Benthos 3.5 KHz Chirp SBP looking at any perfectly straight line of reflection, produced by the sharp salinity : density contrast at the seawater : brine interface. Multibeam swath bathymetry was obtained by the R/V *Urania* Kongsberg-Simrad EM-302 and processed with Neptune, CARIS and GMT packages (Wessel *et al.*, 2013).

### *Sampling of halocline and brine in the Kryos Lake*

Sampling of the *Kryos* Lake was conducted from the RV *Urania* at location (22°01'E 35°02'N – 22°02'E 34°53'N) during two oceanographic cruises in September-October 2008 and September 2009 (Fig.1b). Samples were collected using 12-litre Niskin bottles housed on a rosette (General Oceanics, Inc., Miami, FL, USA) equipped with SBE-911plus conductivity-temperature-depth (CTD) sensors (Sea-Bird Electronics, Inc., Bellevue, WA, USA). Determination of oxygen concentration at chosen depths was carried out using the Winkler method (Carpenter, 1965) with an automatic endpoint detection

1 burette 716 DNS Titrino (Metrohm AG, Herisau, Switzerland). Samples for determining major ion  
2 concentrations were collected in 1000 ml dark polyethylene (DPE) vials and stored at room  
3 temperature. Alternatively, 110 ml of the samples were diluted with double volume of 0.1 M of  $\text{HNO}_3$   
4 and stored in 500 ml DPE vials under room temperature prior the chemical analyses. Samples for  
5 determining nutrient concentrations were collected in 20 ml DPE vials, quickly frozen in liquid  
6 nitrogen and then stored at  $-20^\circ\text{C}$ . Nutrient concentrations were determined within a few weeks of  
7 the end of each cruise using SEAL QuAAtro Microflow Analyzer (SEAL Analytical, Ltd, Hampshire, UK).  
8 All running standards were prepared with Low Nutrient Seawater and calibrated against Ocean  
9 Scientific Standards (OSIL, Hampshire, UK). Sample analyses were performed at least twice using the  
10 same set of equipment. The interface was captured and fractionated as described elsewhere  
11 (Daffonchio *et al.*, 2006; Hallsworth *et al.*, 2007; Yakimov *et al.*, 2013). Briefly, 12-L Niskin bottles  
12 housed on a rosette with a CTD sensors were closed when a large increase in conductivity, indicating  
13 that the interface had been entered, was observed. This was confirmed on-board by measuring the  
14 refractive index of the top and bottom of the brine in the Niskin bottles using a hand refractometer  
15 (Atago, Tokyo, Japan). Fractions (about 0.5 - 2 l) of the captured interface were sub-sampled and  
16 preserved in sealed bottles. Redox potentials (Eh) of subsamples were measured immediately  
17 according to the procedure described by Pearson and Stanley (1979). The samples possessing the  
18 equal values of salinities were pooled for further treatments as reported below. Among all  
19 fractionated samples, the interface layers UIF, CHW and AWW, with salinities of 50-140 PSU, 140-245  
20 PSU and 245-330 PSU, respectively, were subjected to comprehensive analysis of autochthonous  
21 microbial life. Moreover, 5 l of the *Kryos* brine was sampled for comparative purposes from the  
22 depth 3370 m.

23

24 *Geochemical analyses*

1 Dissolved cations, anions and organic acids were quantified from diluted samples using standard ion  
2 chromatographic techniques, as described below. Conductivity measurements of the samples,  
3 determined by a Conductivity meter HI 9818 (Hanna Instruments, Italy), were used to program the  
4 dilution.  $\text{Na}^+$ ,  $\text{K}^+$ ,  $\text{Mg}^{2+}$  and  $\text{Ca}^{2+}$  concentrations were measured using ion exchange chromatography,  
5 with a 761 Compact IC ion chromatography system (Metrohm AG, Switzerland) fitted with Metrosep  
6 C 4 column used without chemical suppression (direct conductivity and reverse polarity modality).  
7 Components were separated using a phosphoric acid (5mM) gradient, with a flow of  $1 \text{ ml min}^{-1}$ .  
8 Volatile fatty acids and sulfate concentrations were measured by ion exchange chromatography  
9 using an ICS-2000 ion chromatography system (Dionex<sup>®</sup>, UK) fitted with two AS15-HC 4 mm columns  
10 in series, and a Dionex<sup>®</sup> Anion Self-Regenerating Suppressor (ASRS<sup>®</sup>-ULTRA II 4-mm) unit in  
11 combination with a Dionex<sup>®</sup>DS6 heated conductivity cell. Components were separated using a  
12 potassium hydroxide gradient program as follows: 6.0 mmol KOH (38 min isocratic), 16.0 mmol KOH  
13  $\text{min}^{-1}$  to 70 mmol (17 min isocratic). For chloride ( $\text{Cl}^-$ ) concentrations, column was exchanged with a  
14 Ionpac AS9-SC. Chloride were separated using a sodium carbonate ( $\text{Na}_2\text{CO}_3$ ) at 2 mmol and sodium  
15 bicarbonate ( $\text{NaHCO}_3$ ) at 0.75 mmol with a flow of  $1.0 \text{ ml min}^{-1}$ .

#### 17 *Extraction of dissolved organic matter*

18 Untreated brine (200 ml) was filtered through pre-combusted Whatman GF/F glass fiber filters.  
19 The pH was adjusted to 2.0 by using high purity grade formic acid (98 %). Solid-phase extraction  
20 (SPE) was followed using Agilent Bond Elut PPL SPE cartridges filled with highly functionalized  
21 styrene-divinylbenzene (SDVB) polymer that has been modified with a proprietary non-polar  
22 surface. The SPE cartridge was activated using methanol (Sigma-Aldrich Chromasolv LC-MS grade  
23 methanol), washed with acidified (pH 2.0) high purity water (Sigma-Aldrich Chromasolv LC-MS  
24 grade water). Then, the acidified sample was gravity-fed through the SPE cartridge. The cartridge  
25 was washed again with acidified pure water to replace the last remaining inorganic ions from the

SPE cartridge. After washing, the cartridge was dried under high purity grade nitrogen gas and eluted with methanol.

#### *Ultrahigh resolution mass spectrometry*

Ultrahigh-resolution mass spectra were acquired on a Bruker (Bremen, Germany) APEX 12 Qe Fourier transform ion cyclotron resonance mass spectrometer equipped with a 12 T superconducting magnet and a APOLLO II electrospray source. The SPE methanol eluate was diluted 1:20 into methanol and introduced into the micro electrospray source at a flow rate of 120 mL/h with a nebulizer gas pressure of 20 psi (138 kPa) and a drying gas pressure of 15 psi (103 kPa) at 250°C through an Agilent sprayer. Spectra were externally calibrated on clusters of arginine (5 mg l<sup>-1</sup> in methanol) and systematically internally calibrated with appropriate reference mass list reaching accuracy values lower than 100 ppb in routine day-to-day measurements. Data acquisition was performed using DataAnalysis associated software (Bruker Daltonics, version 4.0). The possible elemental formulas were calculated from the exported masses list for each peak in batch mode by a software tool written in-house (Netcalc). The generated formulas were validated by setting sensible chemical constraints (N rule, double bond equivalent non-negative integers, O/C ratio  $\leq 1$ , H/C ratio  $\leq 2+2/n$  (where n is the number of carbon). Van Krevelen diagrams (H/C vs O/C) and (H/C vs m/z) diagrams were used to visualize these datasets.

#### *Quantitation of water activity and chaotropic activity*

Besides the natural *Kryos* brine, an artificial analogue brine was also used for water activity and chaotropicity determination. This synthetic, analogue 'Lake *Kryos*' brine was made up by dissolving following salts: MgCl<sub>2</sub> (4.1841 M), MgSO<sub>4</sub> (0.2183 M), Na<sub>2</sub>SO<sub>4</sub> (62 mM) K<sub>2</sub>SO<sub>4</sub> (42.2 mM), CaCl<sub>2</sub> (1 mM), (NH<sub>4</sub>)<sub>2</sub>SO<sub>4</sub> (0.4 mM) which was stored for one week at 14.3°C prior to water-activity determinations.

Water activities were determined over a range of concentrations at 14.3°C using a Novasina IC II water activity machine fitted with an alcohol-resistant humidity sensor and eVALC alcohol filter (Novasina, Pfäffikon, Switzerland), as described previously (Hallsworth and Nomura, 1999). This brine was super-saturated as a fine, powdery precipitate could be seen by eye. For quantification of chaotropic activity, agar gel-points were determined over a range of salt or brine concentrations (see Hallsworth *et al.*, 2003a; 2007) using a Cecil E2501 spectrophotometer fitted with a thermoelectrically controlled heating block (Milton Technical Centre, Cambridge, England) as described previously (Cray *et al.*, 2013a).

#### *CARD-FISH analysis*

CARD-FISH samples (50 ml) were collected from overlying seawater, the interface layers UIF, CHW, AWW and the *Kryos* brine. Samples were fixed with 2% formaldehyde (v/v, final concentration) at room temperature for 1 hour and stored at -20°C in the dark until laboratory analysis. Subsamples (from 1 to 10 ml, according to cell concentrations) were filtered through polycarbonate membranes (Ø25 mm, 0.22 µm pore size, NTG). Cells were permeabilized with lysozyme (10 mg ml<sup>-1</sup>, 1 h) and achromopeptidase (5 mg ml<sup>-1</sup>, 30 min) at 37°C. Intracellular peroxidase was inhibited by treatment with HCl (0.01 mmol l<sup>-1</sup>) at room temperature for 20 min. We used the following horseradish peroxidase labeled probes: EUB338 I-III, ARCH915, CREN537, EURY806, KB1, and Delta-DHAL. Detailed information about the probes shown in Table S1. The nonspecific probe NON338 did not detect any cells. The filters sections were counter-stained with DAPI (2 mg ml<sup>-1</sup>) in a 4:1 ratio of Citifluor (Citifluor Ltd, Leicester, UK) and Vectashield (Linaris GmbH, Wertheim- Bettingen, Germany). At least 200 DAPI cells, in a minimum of 10 fields, were counted in the AXIOPLAN 2 Imaging microscope (Zeiss). Negative control counts were performed with HRP-Non338 probe, always amounting to < 1% of DAPIstained cells.

1    *Nucleic acid purification and cDNA synthesis*

2    For DNA/RNA extraction, 2-5 l of the fractionated interface and brine samples were filtered through  
3    sterile Sterivex capsules (0.2µm pore size, Millipore) using a peristaltic pump. After filtration, filters  
4    were treated with 400µl of TE buffer (pH 8.0) containing lysozyme (5 mg ml<sup>-1</sup>), vortexed for 5 sec and  
5    incubated 10 min at room temperature. 1600µl of lysis buffer QRL1 (containing β-mercaptoethanol)  
6    were added and filters were then stored at -20°C until processing. Total DNA and RNA were  
7    extracted using Qiagen RNA/DNA Mini Kit (Qiagen, Milan, Italy). The extraction was carried out  
8    according to the manufacturer's instructions. DNA and RNA samples were examined by agarose gel  
9    electrophoresis and concentrations were determined using the NanoDrop ND-1000  
10   Spectrophotometer (Wilmington, DE, USA). RNA-containing extracts were purified from DNA by  
11   Turbo DNA-free kit (Ambion, Austin, TX, USA). Each RNA sample was immediately converted into  
12   cDNA with SuperScript II Reverse Transcriptase (Invitrogen, Carlsbad, CA, USA) and hexa-random  
13   primers according to the manufacturer instructions.

14  
15   *PCR-amplification, gene cloning and sequencing*

16   Bacterial 16S *rRNA*, archaeal 16S *rRNA* and key genes involved in sulphur respiration (*dsrAB*) and  
17   methanogenesis (*mcrA*), were amplified by PCR using primers listed in the Table S1. All reactions  
18   were carried out in a MasterCycler 5331 Gradient PCR (Eppendorf, Hamburg, Germany). The  
19   conditions for PCR and cloning were performed as described elsewhere (La Cono *et al.*, 2011,  
20   Yakimov *et al.*, 2013). Positive clones from each library were randomly selected by PCR  
21   amplification. The PCR products were further purified and sequenced at Macrogen (Amsterdam,  
22   Netherlands).

23  
24   *Phylogenetic trees*

1 Pintail software (Ashelford *et al.*, 2005) was used to check sequences for possible chimeric origin.  
2 16S rRNA gene amplified sequences and close relatives identified with BLAST (Altschul *et al.*,  
3 1997) were aligned using the SILVA alignment tool (Pruesse *et al.*, 2007) and manually checked  
4 with ARB (Ludwig *et al.*, 2004). MEGA 5 (Tamura *et al.*, 2007) was used to align functional genes  
5 nucleotides sequences. After alignment, the neighbor-joining algorithm of ARB and MEGA 5  
6 program packages were used to generate the phylogenetic trees based on distance analysis for  
7 16S rRNA and functional genes, respectively. The robustness of inferred topologies was tested by  
8 bootstrap re-sampling using the same distance model (1,000 replicates). Significant difference of  
9 the microbial assemblages derived from different samples depths was detected via the *P*-test  
10 significance and principal coordinates analysis (PCA) using UniFrac program  
11 (<http://bmf2.colorado.edu/fastunifrac> (Hamandy *et al.*, 2009; Lozupone *et al.*, 2007) for  
12 comparison of the microbial communities using phylogenetic information.

13

#### 14 *Nucleotide sequence accession numbers*

15 The nucleotide sequences produced in the present study have been deposited in the  
16 DDBJ/EMBL/GenBank databases under accession numbers: KJ922395 to KJ922487 for the bacterial  
17 and archaeal 16S rRNA gene sequences, KJ922632 to KJ922638 for the archaeal *mcrA* gene  
18 sequence, KJ922623 to KJ922631 for the bacterial *dsrA* gene sequences.

19

#### 20 **Acknowledgements**

21 This work was performed with the financial support of CNR in frames of the EU FP7 Projects MAMBA  
22 (KBBE-2009-2B-226977) and MicroB3 (OCEAN 2011-2-287589). JAC was supported by funding received  
23 from the Department of Agriculture and Rural Development (Northern Ireland). We thank the  
24 Master, crew of RV *Urania* and all participants to the cruises for their valuable professionalism and

support during the cruises. A. Modica, M. Catalfamo are indebted for geochemical analyses. The discoveries were possible only because of good topographic data made available by other Institutions, and we thank Dr. Benoit Loubrieu of IFREMER for providing the 500m-resolution DTM data.

## References

- Altschul, S.F., Madden, T.L., Schäffer, A.A., Zhang, J., Zhang, Z., Miller, W., *et al.* (1997) Gapped BLAST and PSI-BLAST: a new generation of protein database search programs. *Nucleic Acids Res* **25**: 3389–3402.
- Ashelford, K.E., Chuzhanova, N.A., Fry, J.C., Jones, A.J., and Weightman, A.J. (2005) At least 1 in 20 16S rRNA sequence records currently held in public repositories is estimated to contain substantial anomalies. *Appl Environ Microbiol* **71**: 7724–7736.
- Baati, H., Guermazi, S., Gharsallah, N., Sghir, A. and Ammar, E. (2010) Novel prokaryotic diversity in sediments of Tunisian multipond solar saltern. *Res Microbiol* **161**: 573–582.
- Bell, A.N.W., Magill, E., Hallsworth, J.E., and Timson, D.T. (2013) Effects of alcohols and compatible solutes on the activity of  $\beta$ -galactosidase. *Appl Biochem Biotech* **169**: 786–796.
- Bhaganna, P., Volkers, R.J.M., Bell, A.N.W., Kluge, K. Timson, D.J., McGrath, J.W., Ruijsenaarsm H.J., and Hallsworth, J.E, (2010) Hydrophobic substances induce water stress in microbial cells. *Microb Biotechnol* **3**: 701–716.
- Borin, S., Brusetti, L., Mapelli, F., D'Auria, G., Brusa, T., Marzorati, M., *et al.* (2009) Sulfur cycling and methanogenesis primarily drive microbial colonization of the highly sulfidic Urania deep hypersaline basin. *Proc Natl Acad Sci U S A* **106**: 9151–9156.

1 Borrel, G., O'Toole, P.W., Harris, H.M., Peyret, P., Brugère, J.F. and Gribaldo, S. (2013)  
2 Phylogenomic data support a seventh order of methylotrophic methanogens and provide  
3 insights into the evolution of methanogenesis. *Genome Biol Evol* **5**: 1769-1780.

4 Camerlenghi, A. (1990) Anoxic basins of the eastern Mediterranean: geological framework. *Mar*  
5 *Chem* **31**: 1-19.

6 Camerlenghi, A., and McCoy, F.W. (1990) Physiography and structure of Bacino Bannock (Eastern  
7 Mediterranean). *Geo-Mar Lett* **31**: 21-33.

8 Carpenter, A.B. (1978) Origin and chemical evolution of brines in sedimentary basins. *Oklahoma Geol*  
9 *Surv Circ* **79**: 60-77.

10 Chamot-Rooke, N. Rabaute, A., and Kreemer, C. (2005) Western Mediterranean Ridge mud belt  
11 correlates with active shear strain at the prism-backstop geological contact. *Geology* **33**: 861-864.

12 Chin, J.P., Megaw, J., Magill, C.L., Nowotarski, K., Williams, J.P., Bhaganna, P., Linton, M., Patterson,  
13 M.F., Underwood, G.J.C, Mswaka, A.Y., and Hallsworth, J.E. (2010) Solutes determine the  
14 temperature windows for microbial survival and growth. *Proc Natl Acad Sci* **107**: 7835-7840.

15 Cita, M.B. (1991) Anoxic basins of the eastern Mediterranean: An overview. *Paleoceanography* **6**: 133-  
16 141.

17 Cita M.B. (2006) Exhumation of Messinian evaporites in the deep-sea and creation of deep anoxic  
18 brine-filled collapsed basins. *Sediment Geol* **188-189**: 357-378

19 Cray, J.A., Russell, J.T., Timson, D.J., Singhal, R.S., and Hallsworth, J.E. (2013a) An universal  
20 measure of chaotropicity and kosmotropicity. *Environ Microbiol* **15**: 287-296.

21 Cray, J.A., Bell, A.N.W., Bhaganna, P., Mswaka, A.Y., Timson, D.J., and Hallsworth, J.E. (2013b) The  
22 biology of habitat dominance; can microbes behave as weeds? *Microb Biotechnol* **6**: 453-492.

23 Daffonchio, D., Borin, S., Brusa, T., Brusetti, L., van der Wielen, P.W., Bolhuis, H., *et al.* (2006).  
24 Stratified prokaryote network in the oxic-anoxic transition of a deep-sea halocline. *Nature* **440**:  
25 203-207.

- 1 De Lange, G.J. and Ten Haven H.L. (1983) Recent sapropel formation in the eastern Mediterranean.  
2 *Nature* **305**: 797-798.
- 3 De Lange, G.J., Middleburg, J.J., van der Weijden, K.H., Luther III, G.W., Hydes, D.J., Woittiez, J.R.W., *et*  
4 *al.* (1990) Composition of anoxic hypersaline brines in the Tyro and Bannock Basins, Eastern  
5 Mediterranean. *Mar Chem* **31**: 63-88.
- 6 Demergasso, C., Escudero, L., Casamayor, E.O., Chong, G., Balague, V. and Pedros-Alio, C. (2008)  
7 Novelty and spatio-temporal heterogeneity in the bacterial diversity of hypersaline Lake  
8 Tebenquiche (Salar de Atacama). *Extremophiles* **12**: 491-504.
- 9 Dridi, B., Fradeau, M.-L., Ollivier, B., Raoult, D., and Drancourt, M. (2012) *Methanomassiliicoccus*  
10 *luminyensis* gen. nov., sp. nov., a methanogenic archaeon isolated from human faeces. *Int J*  
11 *Syst Evol Microbiol* **62**: 1902-1907.
- 12 Doroshenko, E.A., Zenova, G.M., Zvyagintsev, D.G., and Sudnitsyn, I.I. (2005) Spore germination  
13 and mycelial growth of streptomycetes at different humidity levels. *Mikrobiologiya* **74**: 690-  
14 694.
- 15 Doroshenko, E.A., Zenova, G.M., Sudnicin, I.I., and Zvyagintsev, D.G. (2006) Influence of humidity  
16 on soil mycelial bacteria. *Vestn Mosk U Poch* **1**: 45-48.
- 17 Duda, V.I., Danilevich, V.N., Suzina, N.E., Shorokhova, A.P., Dmitriev, V.V., Mokhova, O.N., and  
18 Akimov, V.N. (2004) Changes in the fine structure of microbial cells induced by chaotropic  
19 salts. *Mikrobiologiya* **73**: 341-349.
- 20 Feike, J., K. Jürgens, J. T. Hollibaugh, S. Krüger, G. Jost and M. Labrenz (2012). Measuring unbiased  
21 metatranscriptomics in suboxic waters of the central Baltic Sea using a new in situ fixation  
22 system. *ISME J* **6**: 461-470.
- 23 Grant, W.D. (2004) Life at low water activity. *Philos Trans R Soc Lond B Biol Sci* **359**: 1249-1266.

1 Grolas, A., Robert, C., Gimenez, G., Drancourt, M. and Raoult D. (2012) Complete genome sequence  
2 of *Methanomassiliicoccus luminyensis*, the largest genome of a human-associated Archaea  
3 species. *J Bacteriol* **194**: 4745.

4 Hallsworth, J.E., and Nomura, N. (1999) A simple method to determine the water activity of  
5 ethanol-containing samples. *Biotechnol Bioeng* **62**: 242–245.

6 Hallsworth, J.E., Heim, S. and Timmis, K.N. (2003a) Chaotropic solutes cause water stress in  
7 *Pseudomonas putida*. *Environ Microbiol* **5**: 1270–1280.

8 Hallsworth, J.E., Prior, B.A., Nomura, Y., Iwahara, M., and Timmis, K.N. (2003b) Compatible solutes  
9 protect against chaotrope (ethanol)-induced, nonosmotic water stress. *Appl Environ Microbiol*  
10 **69**: 7032–7034.

11 Hallsworth, J.E., Yakimov, M.M., Golyshin, P.N., Gillion, J.L., D'Auria, G., de Lima Alves, F., *et al.* (2007)  
12 Limits of life in MgCl<sub>2</sub>-containing environments: chaotropicity defines the window. *Environ*  
13 *Microbiol* **9**: 801-813.

14 Hamady M., Lozupone C.A. and Knight R., (2009) Fast UniFrac: facilitating high-throughput  
15 phylogenetic analyses of microbial communities including analysis of pyrosequencing and  
16 PhyloChip data. *The ISME Journal* (2010) **4**: 17–27.

17 Harrison, J.P., Gheeraert, N., Tsigelnitskiy, D., and Cockell, C.S. (2013) The limits for life under  
18 multiple extremes. *Trends Microbiol* **21**: 204–212.

19 Hertkorn, N., Benner, R., Schmitt-Kopplin, Ph., Kaiser, K., Kettrup, A., Hedges, I.J. (2006)  
20 Characterization of a major refractory component of marine organic matter, *Geochimica*  
21 *Cosmochimica Acta*, **70**: 2990-3010.

22 Jiang, H., Dong, H., Yu, B., Liu, X., Li, Y., Ji, S., *et al.* (2007) Microbial response to salinity change in  
23 Lake Chaka, a hypersaline lake on Tibetan plateau. *Environ Microbiol* **9**: 2603-2621.

- 1 Kurapova, A.I., Zenova, G.M., Sudnitsun, I.I., Kizilova, A.K., Manucharova, N.A., Norovsuren, Zh.,  
2 and Zvyagintsev, D.G. (2012) Thermotolerant and thermophilic actinomycetes from soils of  
3 Mongolia desert steppe zone. *Microbiology* **81**: 98–108.
- 4 La Cono V, Smedile F, Bortoluzzi G, Arcadi, E., Maimone, G., Messina, E. et al. (2011) Unveiling  
5 microbial life in new deep-sea hypersaline Lake Thetis. Part I: Prokaryotes and environmental  
6 settings. *Environm Microbiol* **13**: 2250–2268.
- 7 Lievens, B., Hallsworth J.E., Belgacem, Z.B., Pozo, M.I., Stevenson, A., Willems, K.A., and H. Jacquemyn  
8 (2014) Microbiology of sugar-rich environments: diversity, ecology, and system constraints.  
9 *Environmental Microbiology Reports* (in press).
- 10 Loubrieu B., Mascle J. Benkhelil, J., Bernè, S., Chamot-Rooke, N., Deverchère, J. *et al.* (2008) Morpho-  
11 bathymetry of the Mediterranean Sea, CIESM/Ifremer Medimap Group, CIESM edition.
- 12 Lozupone, C.A., Hamady, M., Kelley, S.T. and Knight, R. (2007) Quantitative and qualitative beta  
13 diversity measures lead to different insights into factors that structure microbial communities.  
14 *Appl Environ Microbiol* **73**: 1576–1585.
- 15 Ludwig, W., Strunk, O., Westram, R., Richter, L., Meier, H., Yadhukumar, B., *et al.* (2004) ARB: a  
16 software environment for sequence data. *Nucleic Acids Res* **32**: 1363–1371.
- 17 Makhdoumi-Kakhki, A., Amoozegar, M.A., Kazemi, B., Pasic, L. and Ventosa, A. (2012) Prokaryotic  
18 diversity in Aran-Bidgol Salt Lake, the largest hypersaline Playa in Iran. *Microbes Environ* **27**: 87-  
19 93.
- 20 Marion, G.M., Fritsen, C.H., Eicken, H., and Payne, M.C. (2003) The search for life on Europa:  
21 limiting environmental factors, potential habitats, and earth analogues. *Astrobiol* **3**: 785–811.
- 22 McCaffrey, M.A., Lazar, B. and Holland, H.D., (1987) The evaporation path of seawater and the  
23 coprecipitation of Br<sup>-</sup> and K<sup>+</sup> with halite. *J Sediment Petrol* **57**: 928–937.

- 1 MEDRIFF Consortium (1995) Three brine lakes discovered in the seafloor of the eastern  
2 Mediterranean. *EOS Trans AGU* **76**: 313.
- 3 Oren, A. (1983) *Halobacterium sodomense* sp. nov., a Dead Sea *Halobacterium* with an extremely  
4 high magnesium requirement. *Int J Syst Bacteriol* **33**: 381–386.
- 5 Oren, A. (1999) Bioenergetic aspects of halophilism. *Microbiol Mol Biol Rev* **63**: 334–348.
- 6 Oren, A. (2010) The dying Dead Sea: the microbiology of an increasingly extreme environment.  
7 *Lakes Reser: Res Manag* **15**: 215–222.
- 8 Pearson, T.H., and Stanley, S.O. (1979) Comparative measurements of the redox potential of  
9 marine sediments as a rapid means of assessing the effect of organic pollution. *Mar Biol* **53**:  
10 371–379.
- 11 Pitt, J.I. and Christian, J.H.B. (1968) Water relations of xerophilic fungi isolated from prunes. *Appl*  
12 *Environ Microbiol* **16**: 1853–1858.
- 13 Pitt, J.I. (1975) Xerophilic fungi and the spoilage of foods of plant origin. In *Water Relations of*  
14 *Foods*. Duckworth, R.B. (ed.). London, United Kingdom: Academic Press, pp. 273–307.
- 15 Potts M (1994) Desiccation tolerance of prokaryotes. *Microbiol Rev* **58**:755–805.
- 16
- 17 Pruesse, E., Quast, C., Knittel, K., Fuchs, B.M., Ludwig, W., Peplies, J., *et al.* (2007) SILVA: a  
18 comprehensive online resource for quality checked and aligned ribosomal RNA sequence data  
19 compatible with ARB. *Nucleic Acids Res* **35**: 7188–7196.
- 20 Raup, O.B. (1970) Brine mixing: An additional mechanism for the formation of evaporate brines.  
21 *Bulletin of the American Association of Petroleum Geologists* **54**: 2246–2259.

1 Tamura, K., Peterson, D., Peterson, N., Stecher, G., Nei, M., and Kumar, S. (2011) MEGA5: molecular  
2 evolutionary genetics analysis using maximum likelihood, evolutionary distance, and  
3 maximum parsimony methods. *Mol Biol Evol* **28**: 2731–2739.

4 Schmitt-Kopplin, Ph., Gelencser, A., Dabek-Zlotorzynskaya, E., Kiss, G., Hertkorn, N., Harir, *et al.*  
5 (2010a) Analysis of the unresolved organic fraction in atmospheric aerosols with ultrahigh-  
6 resolution mass spectrometry and nuclear magnetic resonance spectroscopy: organosulfates  
7 as photochemical smog constituents. *Anal Chem* **82**: 8017-8016.

8 Schmitt-Kopplin, Ph., Gabelica, Z., Gougeon, R.D., Fekete, A., Kanawati, B., Harir, M. *et al.* (2010b)  
9 High molecular diversity of extraterrestrial organic matter in Murchison meteorite revealed  
10 40 years after its fall. *PNAS* **107**: 2763-2768.

11 Stevenson, A. and Hallsworth, J.E. (2014) Water and temperature relations of soil Actinobacteria.  
12 Revised for *Environmental Microbiology Reports*.

13 Stevenson, A., Burkhardt, J., Cockell, C.S., Cray, J.A., Fox-Powell, M., Kee, T.P., *et al.* (2014)  
14 Multiplication of microbes below 0.690 water activity: implications for terrestrial and  
15 extraterrestrial life. Under revision for *Environmental Microbiology*.

16 van der Wielen, P.W., H. Bolhuis, J.J., Borin, S., Daffonchio, D., Corselli, C., Giuliano, L., *et al.* (2005)  
17 The enigma of prokaryotic life in deep hypersaline anoxic basins. *Science* **307**: 121-123.

18 Wallmann, K.J., Suess, E., Westbrook, G.H., Winckler, G., Cita, M.B., and the Medriff consortium (1997)  
19 Salty brines on the Mediterranean sea floor. *Nature* **387**: 31-32.

20 Wallmann, K., Aghib, F.S., Castradori, D., Cita, M.B., Suess, E., Greinert, J., and Rickert, D. (2002)  
21 Sedimentation and formation of secondary minerals in the hypersaline Discovery Basin, eastern  
22 Mediterranean. *Mar Geol* **186**: 9–28.

23 Wessel, P., Smith, W.H.F., Scharroo, R., Luis, J.F. and Wobbe F. (2013) Generic mapping tools:  
24 improved version released, *EOS Trans AGU* **94**: 409-410.

1 Williams, J.P., and Hallsworth, J.E. (2009) Limits of life in hostile environments; no limits to  
2 biosphere function? *Environ Microbiol* **11**: 3292–3308.

3 Winston, P.W. and Bates, P.S. (1960) Saturated salt solutions for the control of humidity in  
4 biological research. *Ecology* **41**: 232–237.

5 Yakimov, M.M., La Cono, V., Denaro, R., D'Auria, G., Decembrini, F., Timmis, K.N., *et al.* (2007a)  
6 Primary producing prokaryotic communities of brine, interface and seawater above the halocline  
7 of deep anoxic lake L'Atalante, Eastern Mediterranean Sea. *Int Soc Microb Ecol J* **1**: 743–755.

8 Wyatt, T.T., Golovina, E.A., van Leeuwen, M.R., Hallsworth, J.E., Wösten, H.A.B. and J. Dijksterhuis  
9 (2014a) Decreases in bulk water and mannitol and accumulation of trehalose and trehalose-  
10 based oligosaccharides define a two-stage maturation process towards extreme stress-  
11 resistance in ascospores of *Neosartorya fischeri* (*Aspergillus fischeri*). *Environmental*  
12 *Microbiology* In press (doi: 10.1111/1462-2920.12557).

13 Wyatt, T.T., van Leeuwen, M.R., Gerwig, G.J., Golovina, E.A., Hoekstra, F.A., Kuenstner, E.J., *et al.*  
14 (2014b) Functionality and prevalence of trehalose-based oligosaccharides as novel compatible  
15 solutes in ascospores of *Neosartorya fischeri* (*Aspergillus fischeri*) and other fungi.  
16 *Environmental Microbiology* In press (doi: 10.1111/1462-2920.12558).

17

18 Yakimov, M.M., Giuliano, L., Cappello, S., Denaro, R., and Golyshin, P.N. (2007b) Microbial Community  
19 of a Hydrothermal Mud Vent Underneath the Deep-Sea Anoxic Brine Lake Urania (Eastern  
20 Mediterranean). *Orig Life Evol Biosph* **37**: 177–188.

21 Yakimov, M.M., La Cono, V., Slepak, V.Z., La Spada, G., Arcadi, E., Messina, E., *et al.* (2013) Microbial  
22 life in the Lake *Medee*, the largest deep-sea salt-saturated formation. *Sci Report* **3**: 3554

23 Zvyagintsev, D.G., Zenova, G.M., Doroshenko, E.A., Gryadunova, A.A., Gracheva, T.A., and  
24 Sudnitsyn, I.I. (2007) Actinomycete growth in conditions of low moisture. *Izv Akad Nauk Ser*  
25 *Biol* **34**: 242–247.

1 Zvyagintsev, D.G., Zenova, G.M., Sudnitsyn, I.I., Gracheva, T.A., Napol'skaya, K.R., and Belousova,  
2 M.A. (2009) Dynamics of spore germination and mycelial growth of streptomycetes under low  
3 humidity conditions. *Microbiology* **78**: 440–444.  
4 Zvyagintsev, D.G., Zenova, G.M., Sudnitsyn, I.I., Gracheva, T.A., Lapygina, E.E., Napol'skaya, K.R.,  
5 and Sydnitsyna, A.E. (2012) Development of actinomycetes in brown semidesert soil under low  
6 water pressure. *Eurasian Soil Sci* **45**: 717–725.  
7

1  
2 **Table 1.** Chemical composition of the three saltiest DHALs on Earth.

	DISCOVERY*	KRYOS	L'ATALANTE
Salinity, g kg <sup>-1</sup>	510	471	352
Distance of lake surface to bsl, m	3580	3337	3428
Brine depth, m	55	160	80
Brine temperature, °C	16.1	14.5	14.3
Density, kg l <sup>-1</sup>	1.33	1.31	1.23
Na, g kg <sup>-1</sup>	1.93	2.84	107
Cl, g kg <sup>-1</sup>	360	321	188
Mg, g kg <sup>-1</sup>	125	107	16
K, g kg <sup>-1</sup>	3.5	3.3	14.4
Ca, g kg <sup>-1</sup>	0.04	0.04	0.3
SO <sub>4</sub> , g kg <sup>-1</sup>	10.6	31	32
Br, g kg <sup>-1</sup>	8.81	5.60	0.49
ΣO <sub>2</sub> , g kg <sup>-1</sup>	0.18	0.66	1.54
Li, mg kg <sup>-1</sup>	4.9	3.7	0.5
H <sub>2</sub> S, mg kg <sup>-1</sup>	29	41	96
NH <sub>4</sub> , mg kg <sup>-1</sup>	11	16	52
B, mg kg <sup>-1</sup>	283	362	13.2
PO <sub>4</sub> , mg kg <sup>-1</sup>	5.6	6.8	1.2

3  
4 These data were partially taken from Wallmann *et al.* 1997, 2002.

**Table 2.** Chemical compositions of the most anhydrous ( $A_w < 0.700$ ) athalassohaline lakes on Earth and primary (LSPB) and secondary (SB) brines. All concentrations are in mM ( $\text{kg H}_2\text{O}$ )<sup>-1</sup> unless otherwise stated.

	LSPB <sup>a</sup>	SB <sup>b</sup>	DEAD SEA <sup>c</sup>	DON JUAN POND <sup>c</sup>	DISCOVERY	KRYOS
Major ions, mM kg <sup>-1</sup>						
Na	166	99	1835	112	84	125
Mg	5410	5410	1944	110	5150	4379
K	71	112	212	8	90	80
Ca	1	3	459	5830	1	1
SO <sub>4</sub>	173	122	6	<1	110	320
Cl	10100	10926	6824	12192	10150	9043
Parameters						
pH	~5.6 <sup>a</sup>	~5.6 <sup>a</sup>	7.7	~5.4 <sup>a</sup>	~4.5 <sup>a</sup>	~5.4 <sup>a</sup>
Water activity, $A_w$	<b>0.420</b>	<b>0.380</b>	0.690	<b>0.411</b>	<b>0.382</b>	<b>0.399</b>
Salinity, g kg <sup>-1</sup>	513	515	359	670	510	471
Density, kg L <sup>-1</sup>	1.33	1.33	1.22	1.39	1.33	1.32

<sup>a</sup> As it described elsewhere (Wallmann *et al.*, 1997, 2002), the late stage primary brine (LSPB) was produced by evaporation of seawater and precipitation of anhydrite (CaSO<sub>4</sub>), halite (NaCl), kieserite (MgSO<sub>4</sub>·H<sub>2</sub>O) and carnallite (KMgCl<sub>3</sub>·6H<sub>2</sub>O). The evaporation was performed at atmospheric pressure and 30°C and continued until only 5g of the initial 1 kg H<sub>2</sub>O remained in solution.

<sup>b</sup> Secondary brine (SB) produced by equilibrating of calcite-saturated seawater with the evaporite minerals bischofite (MgCl<sub>2</sub>·6H<sub>2</sub>O), kainite (KMg(SO<sub>4</sub>)Cl·3H<sub>2</sub>O), halite, and gypsum (CaSO<sub>4</sub>·2H<sub>2</sub>O) at 14°C and 1 atm (Wallmann *et al.*, 2002).

<sup>c</sup>Composition of the Dead Sea (Israel) and the Don Juan Pond (Antarctica) were taken from Marion *et al.* 2003. Water activity values below the window of cellular life ( $A_w < 0.605$ ) are highlighted in bold.

**Table 3.** Abundance of general and specific phylogenetic groups within *Bacteria* and *Archaea* in the *Kryos* interface layers and overlaying seawater.

The total cell numbers are given as  $10^5$  cells  $\text{ml}^{-1}$  unless otherwise stated. Cells were collected from the indicated layers and hybridized with the specific CARD-FISH probes (Yakimov *et al.*, 2013).

Interface layer <sup>a</sup> , ( $\text{Mg}^{2+}$ , M / salinity, PSU)	DAPI	EUB338 I-III	KB1	Delta-DHAL	ARCH915	CREN537	EURY806
SW <sup>b</sup>	0.16±0.02	0.12±0.02	0	0	0.02±0.008	0.02±0.004	0
UIF (0.16/52)	0.93±0.10	0.32±0.08	0	0	0.17±0.05	0.16±0.02	0.02±0.01
CHW (1.55/195)	5.57±0.45	2.97±0.56	0.17±0.03	0.14±0.04	0.81±0.77	0.05±0.01	0.22±0.01
AWW1 (3.03/327)	4.60±0.43	2.45±0.21	0.69±0.12	0.14±0.03	0.43±0.07	0	0
AWW2 (3.41/370)	2.47±0.11	1.53±0.07	1.22±0.11	0.13±0.01	0.47±0.05	0	0

<sup>a</sup> See Figure 2 for exact positioning of sampling points within three layers of the *Kryos* interface.

<sup>b</sup> These data correspond to the seawater column sampled from the depth of 2850 m twenty nautical miles NE from the Lake *Kryos* during the same cruise as it described elsewhere (La Cono *et al.* 2011).

## Figure legends

**Figure 1.** Location of currently known DHALs in the Eastern Mediterranean Sea (a) and the detailed swath bathymetry at the *Kryos* Lake area (b).

The map to the left was constructed using the Ocean Data View software (Schlitzer *et al.*, 2010). On the right, the shape of the anoxic lake and small polar satellite pools are colored in blue starting from the seawater : brine lake interface (3337 m depth). The sampling sites are highlighted by asterisks.

**Figure 2.** Physicochemical activities of  $\text{MgCl}_2$  solutions, the Lake *Kryos* brine and a synthetic *Kryos*-brine analogue: (a) water-activity reduction over a range of  $\text{MgCl}_2$  concentrations at 14.3°C (for comparative purposes all values are expressed according to their  $\text{MgCl}_2$  content) and the upper dotted line indicates the lower boundary of the previously established chaotropy limit of life (CHW, equivalent to 2.3 M  $\text{MgCl}_2$ ; Hallsworth *et al.*, 2007) and the lower dotted line denotes the established water-activity limit for xerophilic fungi (AWW; Pitt and Christian, 1968); and (b) agar gel-point depression (a measure of chaotropic activity; Cray *et al.*, 2013a).

The solid lines with arrows indicate the water-activity values corresponding to the AWW layer ( $\text{MgCl}_2$  2.27 - 3.03 M).

**Figure 3.** Depth profiles of geochemical markers through the Lake *Kryos* and the established boundary for chaotropy and xerophilic cellular life occurred in the *Kryos* gradient.

As far as all conventional on-line CTD sensors were not functional in  $\text{MgCl}_2$ -rich ambience, chemical analysis of fractionated interface samples were performed in the in-land laboratory. The brine was collected at the depths of 3340 and 3370 m bsl. The layers of interface collected for the molecular

analyses are highlighted in green, blue and red. Following the  $A_w$  calculations (Fig. 2a), the boundary for chaotropy ( $A_w$  0.790) and xerophilic cellular life ( $A_w$  0.605) occurred in the *Kryos* gradient are shown. Abbreviations used: AWW, the interface layer corresponding to lower boundary of estimated xerophilic cellular life; BB, body brine; CHW, the interface layer corresponding to lower boundary of chaotropy life; UIF, upper interface. Data points are mean  $\pm$  standard error (n=3).

**Figure 4.** Ultrahigh resolution mass spectrometry of the *Kryos* brine DOM showing hundreds of low molecular weight organic compounds (a) with  $m/z$  <500 amu. The van Krevelen diagrams (b, c) illustrate the high proportion of largely saturated structures and the remarkable extent of oxygenation of the CHNO and poly-sulfur compounds (d). The blue line refers to any fully saturated open chain aliphatic (poly)carboxylic acid, (comparable to polymaleic acid or polyacrylic acid as model structures) and the red line to the compositional range of CRAM molecules as described in Hertkorn *et al.* (2006).

**Figure 5.** Overview on prokaryotic diversity, stratification (a) and relative abundance (b) of phylogenetic groups recovered from the different compartments of Lake *Kryos*.

(a) Stratification and relative abundance of each phylogenetic group found in different layers of the Lake *Kryos* is shown as number of cloned and analysed sequences related to the indicated group. The clones recovered from the *Kryos* brine, the upper interface (UIF), the layer of chaotropy (CHW) and the water activity (AWW) windows are shown in black, green, blue and red, respectively. Scale bar corresponds to 10% estimated difference in nucleotide sequence positions.

(b) Extent of recovery of 16S crDNA AWW clone sequences in overlaying layers UIF and CHW. Scale white bar corresponds to 20% of all cloned sequences analyzed separately in UIF, CHW and AWW clone libraries. Exact percentages of clones corresponding to each indicated phylogenetic group are given for clarity.

Abbreviations of candidate division used: BRC1, Bacterial Rice Cluster; DP, Deltaproteobacteria; HA, haloarchaea; HC1, Halophilic Cluster 1; KB1, Kebrit Deep Bacteria 1; MH, *Methanohalophilus*; MSBLx, Mediterranean Sea Brine Lakes; OM27, Ocean Margins 27; SA1, Shaban Deep Archaea 1; SARx, Sargasso Sea Clusters.

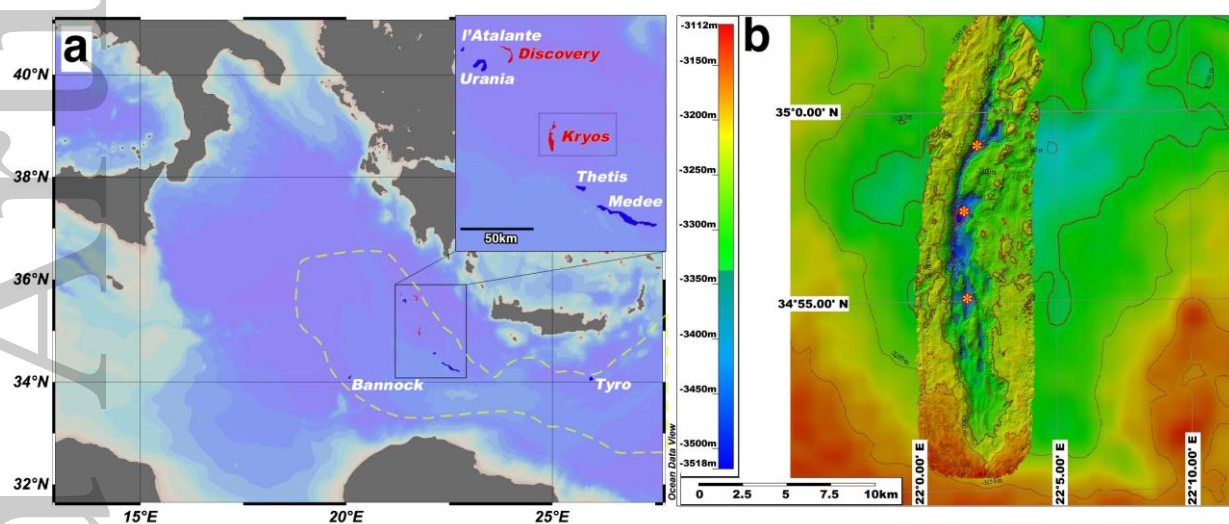
**Figure 6.** Phylogenetic analyses of clone sequences of Archaea and *mcrA* gene transcripts recovered from the AWW interface layer.

The 16S rRNA phylogenetic analysis indicates the relationship between AWW archaeal clone sequences and related sequences recovered from the CHW interface layer, the *Kryos* brine and other DHALs and surficial hypersaline lakes. The analysis of sequences derived from mRNA coding for methyl co-M reductase (*mcrA*) indicates that methanogens similar to both the lake *Discovery* organisms and *Methanohalophilus halophilus* are active in the AWW layer. The white and solid cycles at the nodes indicate the percentages of recovery in 1,000 bootstrap resamplings of < 75% and  $\geq 75\%$ , respectively. Only relevant bootstrap values of  $\geq 70\%$  are shown. Scale bar corresponds to 5% estimated difference in nucleotide sequence positions. Trees were respectively rooted with *Desulfotignum balticum* 16S rRNA (AF233370) and *Methanobrevibacter arboriphilus* DSM 1125 *mcrA* (AF414035) gene sequences.

**Figure 7.** Phylogenetic analysis of bacterial clone sequences and *dsrAB* gene transcripts recovered from the AWW interface layer.

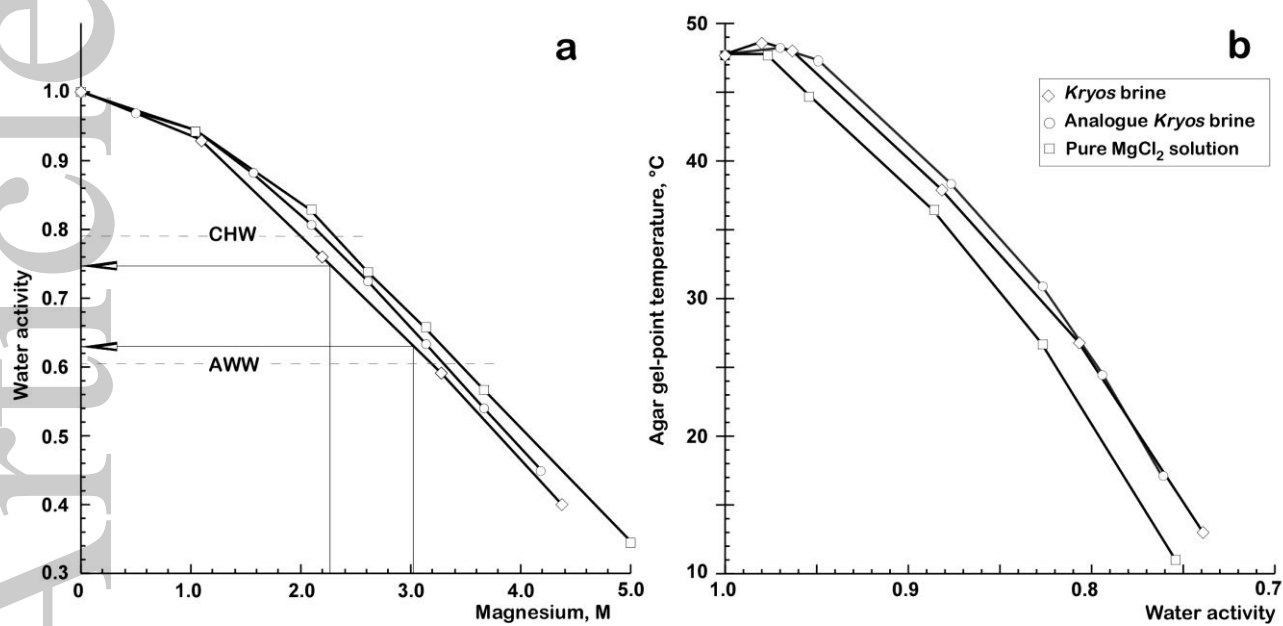
The phylogenetic analysis indicates the relationship between AWW bacterial clone sequences and related sequences recovered from the CHW interface layer, the *Kryos* brine and other DHALs and surficial hypersaline lakes. It also demonstrates that a taxonomic (16S rRNA) and a functional (*dsrAB*) marker give largely congruent phylogenies and the main taxa identified were

1 *Desulfobacteraceae* and *Desulfohalobiaceae*. The white and solid cycles at the nodes indicate the  
 2 percentages of recovery in 1,000 bootstrap resamplings of  $< 75\%$  and  $\geq 75\%$ , respectively. Only  
 3 relevant bootstrap values of  $\geq 70\%$  are shown. Scale bar corresponds to 5% estimated difference in  
 4 nucleotide sequence positions. Trees were respectively rooted with *Halorhabdus tiamatea* 16S rRNA  
 5 (NR\_113213) and *Thermodesulforhabdus norvegica* *dsrAB* (AF334597) gene sequences.



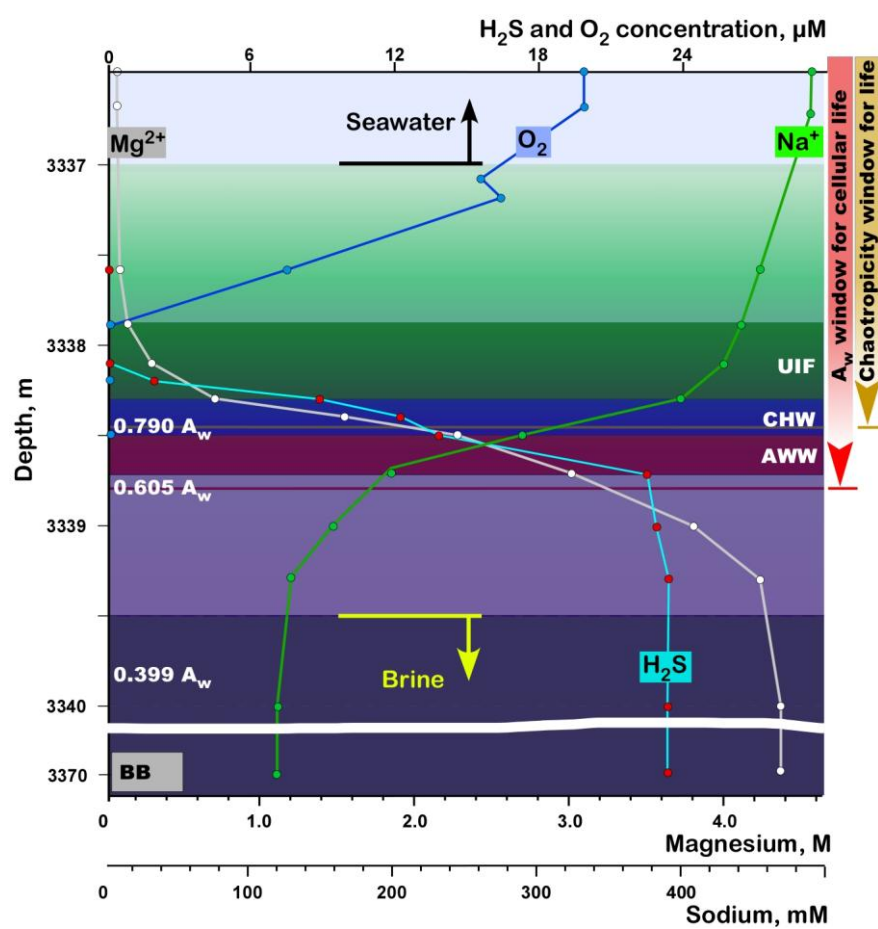
emi\_12587\_f1

1

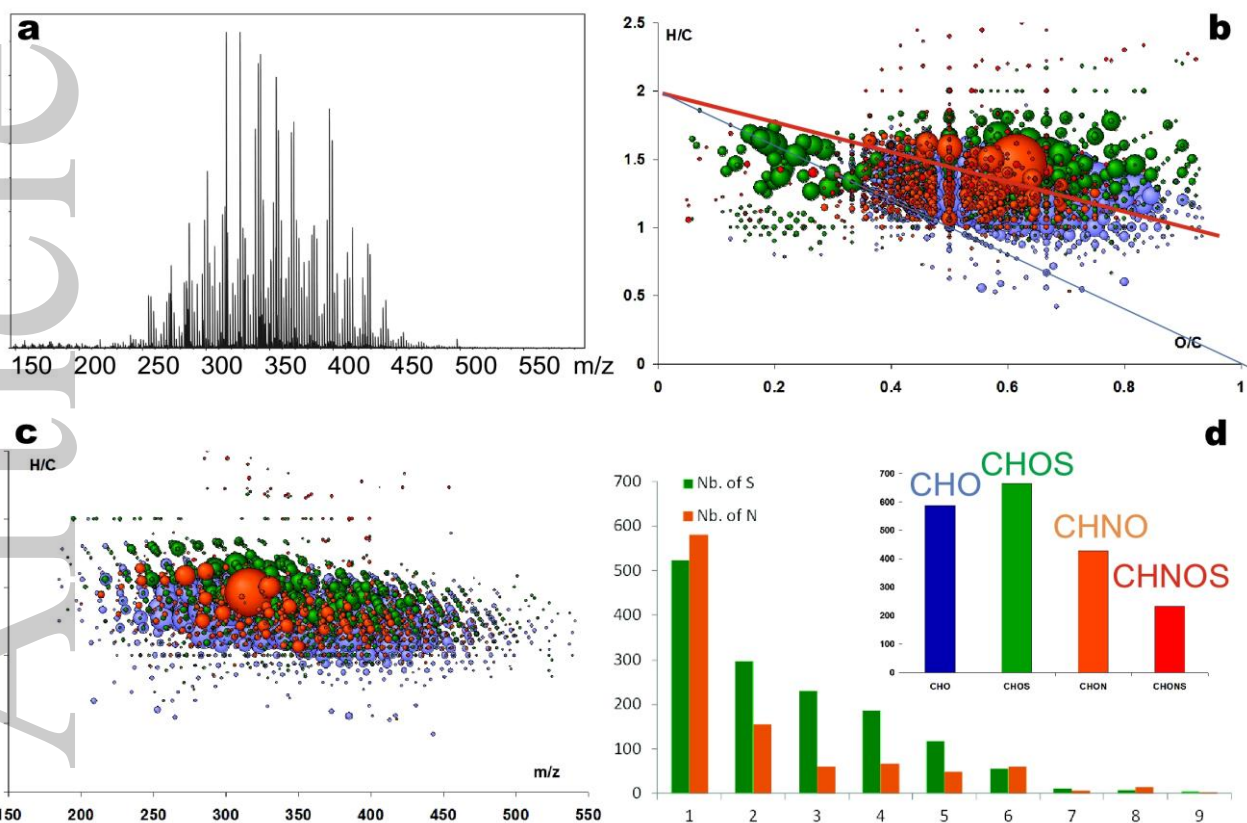


emi\_12587\_f2

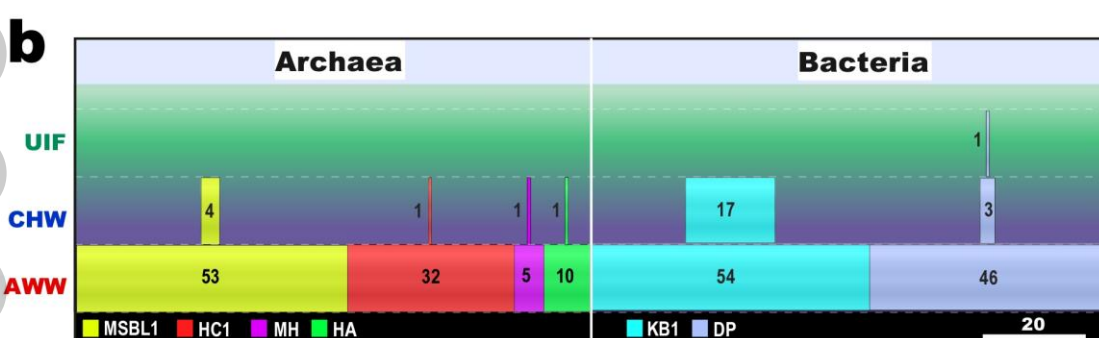
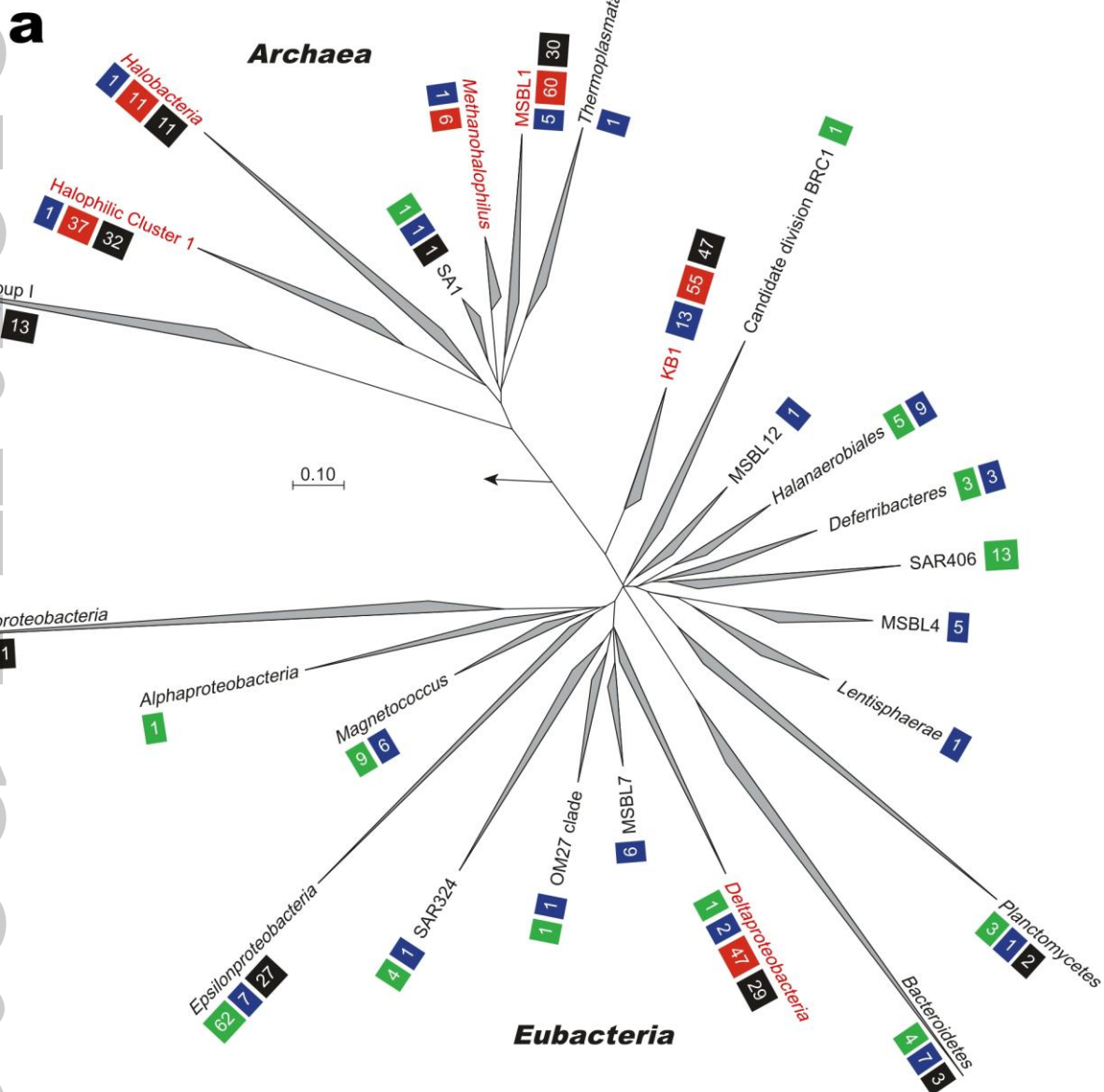
1



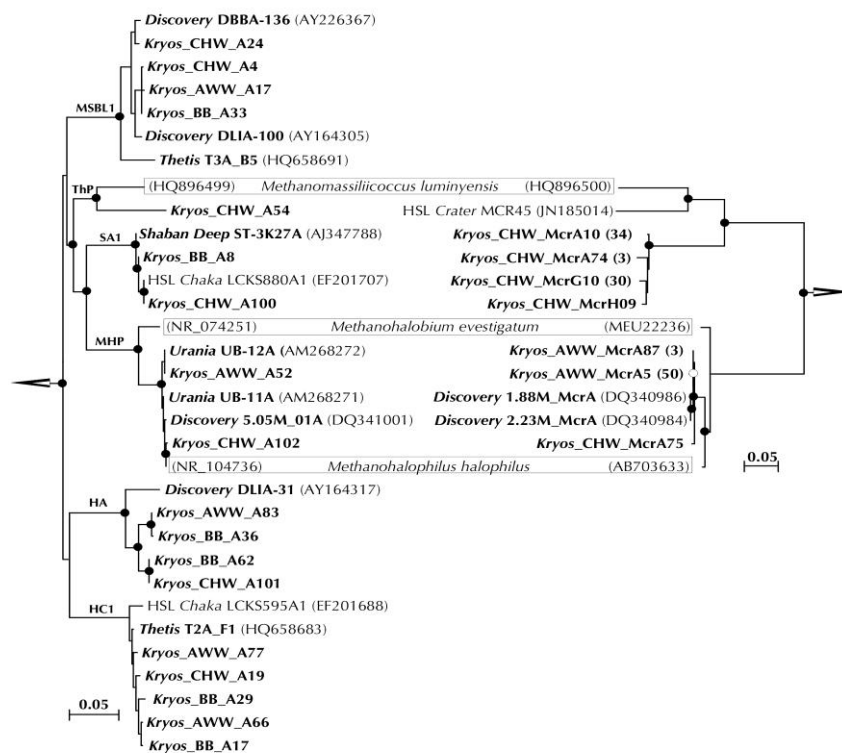
emi\_12587\_f3



emi\_12587\_f4



emi\_12587\_f5



emi\_12587\_f6

